

# VIEWING DETERMINANTS AS NONINTERSECTING LATTICE PATHS YIELDS CLASSICAL DETERMINANTAL IDENTITIES BIJECTIVELY

MARKUS FULMEK

**ABSTRACT.** In this paper, we show how general determinants may be viewed as generating functions of nonintersecting lattice paths, using the Lindström–Gessel–Viennot–interpretation of semistandard Young tableaux and the Jacobi–Trudi identity together with elementary observations. After some preparations, this point of view provides very simple “graphical proofs” for classical determinantal identities like the Cauchy–Binet formula, Dodgson’s condensation formula, the Plücker relations and Laplace’s expansion. Also, a determinantal identity generalizing Dodgson’s condensation formula is presented, which might be new.

## 1. INTRODUCTION

In [2], a combinatorial proof was given for two Schur function identities, which were presented in [8] and in [9]. This combinatorial proof was shown to apply to a *class* of Schur function identities [2, Lemma 16], and was used to prove bijectively Dodgson’s condensation formula and the Plücker relations for examples, but was not paid further attention. Recently, members of this class of Schur function identities received some interest [5]. The close connection of the result [5, (3.3)] was already explained *ad hoc* in [1], but we take this opportunity to make obvious the much wider range of applicability of this idea, which amounts to “viewing determinants as (generating functions of) nonintersecting lattice paths”, by giving concrete examples. The combinatorial constructions are best conceived by pictures, so we give a lot of illustrations.

This paper is organized as follows:

In Section 2, we present basic background information regarding symmetric functions, partitions, Young tableaux and (skew) Schur functions.

In Section 3, we present the Lindström–Gessel–Viennot–interpretation of semistandard Young tableaux as nonintersecting lattice paths, and illustrate this view by giving a “graphical proof” of the Cauchy–Binet formula.

In Section 4, we present the central bijective construction (recolouring of bicoloured trails in the overlays of families of nonintersecting lattice paths corresponding to some product of skew Schur functions) and indicate how this construction applies to a class of Schur function identities.

---

*Date:* October 20, 2010.

Research supported by the National Research Network “Analytic Combinatorics and Probabilistic Number Theory”, funded by the Austrian Science Foundation.

In Section 5, we present several examples: We prove a generalization of Dodgson's condensation rule which might be new (Theorem 2) and give “graphical proofs” for the Plücker relations (and its generalization [5, (3.3)]) and for (a generalization of) Laplace's expansion.

## 2. BASIC DEFINITIONS

The notation  $|x|$  has three different meanings in our presentation, depending on the type of object  $x$  (the respective meaning should always be clear from the context):

- if  $x$  is a *set*, then  $|x|$  denotes the *cardinality* of  $x$ ,
- if  $x$  is a *matrix*, then  $|x|$  denotes the *determinant* of  $x$ ,
- if  $x$  is a *partition* or *shape*, then  $|x|$  denotes the *sum of parts* of  $x$  (to be explained below).

In the following, we shall briefly recall basic concepts and facts needed for our presentation. (More information can be found, e.g., in [11].)

**2.1. The ring of symmetric functions.** Consider the ring  $\mathbb{Z}[x_1, x_2, \dots, x_n]$  of polynomials in  $n$  independent variables  $\mathbf{x} := (x_1, x_2, \dots, x_n)$  with integer coefficients. The *degree* of a monomial  $x_1^{k_1} \cdot x_2^{k_2} \cdots x_n^{k_n}$  is the sum  $k_1 + k_2 + \cdots + k_n$ , and a polynomial  $p$  is called *homogeneous* of degree  $k$  if all monomials of  $p$  have the same degree  $k$ .

The symmetric group  $\mathfrak{S}_n$  acts on this ring by permuting the variables, and a polynomial is *symmetric* if it is invariant under this action. The set of all symmetric polynomials forms a subring  $\Lambda_n \subseteq \mathbb{Z}[x_1, x_2, \dots, x_n]$  which is *graded*, i.e.,

$$\Lambda_n = \bigoplus_{k \geq 0} \Lambda_n^k,$$

where  $\Lambda_n^k$  consists of the homogeneous symmetric polynomials of degree  $k$ , together with the zero polynomial.

For each  $r \in \mathbb{Z}$ , the *complete symmetric function*  $h_r(\mathbf{x})$  is the sum of all monomials of degree  $r$ . In particular,  $h_0(\mathbf{x}) = 1$  and, by convention,  $h_r(\mathbf{x}) = 0$  for  $r < 0$ .

For example, if  $n = 3$ , then  $\mathbf{x} = (x_1, x_2, x_3)$  and

$$h_2(x_1, x_2, x_3) = x_1^2 + x_2^2 + x_3^2 + x_1x_2 + x_1x_3 + x_2x_3.$$

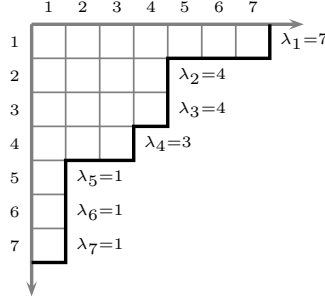
The following fact is well-known (see, e.g., [11, (2.8)]):

**Proposition 1.** *The set of all homogeneous symmetric functions is algebraically independent, i.e.,  $p \equiv 0$  is the only polynomial such that  $p(h_0(\mathbf{x}), h_1(\mathbf{x}), \dots) \equiv 0$ .*

Moreover, for  $0 < k < n$ , the set

$$\{h_i(x_1, \dots, x_k) : i = 0, 1, 2, \dots\} \cup \{h_i(x_{k+1}, \dots, x_n) : i = 1, 2, 3, \dots\}$$

is also algebraically independent. □

FIGURE 1. Illustration: Ferrers diagram  $F_\lambda$  of the partition  $\lambda = (7, 4, 4, 3, 1, 1, 1)$ .

**2.2. Schur functions.** Recall the following standard definitions: An infinite weakly decreasing series of nonnegative integers  $\lambda = (\lambda_i)_{i=1}^\infty$ , where only finitely many elements are positive, is called a *partition*. The largest index  $i$  for which  $\lambda_i > 0$  is called the *length* of the partition  $\lambda$  and is denoted by  $\ell(\lambda)$ . The sum of the non-zero parts  $\lambda_1 + \lambda_2 + \cdots + \lambda_{\ell(\lambda)}$  of  $\lambda$  is denoted by  $|\lambda|$ . In most cases we shall omit the trailing zeroes, i.e., for  $\ell(\lambda) = r$  we simply write  $\lambda = (\lambda_1, \lambda_2, \dots, \lambda_r)$ , where  $\lambda_1 \geq \lambda_2 \geq \cdots \geq \lambda_r > 0$ .

For example,  $\lambda = (7, 4, 4, 3, 1, 1, 1)$  is a partition of length  $\ell(\lambda) = 7$  with  $|\lambda| = 21$ .

The *Ferrers diagram*  $F_\lambda$  of  $\lambda$  is an array of cells with  $\ell(\lambda)$  left-justified rows and  $\lambda_i$  cells in row  $i$ . For an illustration, see Figure 1.

For our purposes, it is convenient to generalize this definition: By a *semipartition* we understand an infinite weakly decreasing series of integers  $(\lambda_i)_{i=1}^\infty$ , where

$$\lambda_\infty := \lim_{n \rightarrow \infty} \lambda_n > -\infty.$$

The length of semipartition  $\lambda$  is the largest integer  $m$  with  $\lambda_m > \lambda_\infty$ , which we denote again by  $\ell(\lambda)$ : Note that every partition  $\mu$  is a semipartition with  $\mu_\infty = 0$ .

Clearly, the set of semipartitions is closed under component-wise addition

$$\lambda + \mu = (\lambda_i)_{i=1}^\infty + (\mu_i)_{i=1}^\infty := (\lambda_i + \mu_i)_{i=1}^\infty.$$

For  $m, z \in \mathbb{Z}$ ,  $m > 0$ , denote by  $(z)$  and  $(z^{(m)})$  the semipartitions

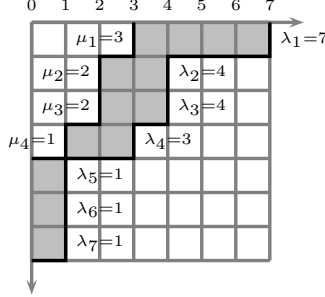
$$(z) := (z)_{i=1}^\infty \quad \text{and} \quad (z^{(m)}) := \left( \underbrace{z, z, \dots, z}_{m \text{ times}}, 0, 0, \dots \right),$$

respectively. (Note that  $(z^{(m)})_\infty = 0$ .) If two semipartitions  $\lambda, \mu$  satisfy

- $\mu_i \leq \lambda_i$  for all  $i = 1, 2, \dots$ ,
- $\mu_\infty = \lambda_\infty$ ,

then we denote this by  $\mu \leq \lambda$  and introduce the symbol  $\lambda/\mu$ , which we call a *shape*. The length of the shape  $\lambda/\mu$  is defined by  $\ell(\lambda/\mu) := \ell(\lambda)$ , and the (terminating!) sum  $\sum_{i=1}^\infty (\lambda_i - \mu_i)$  is denoted by  $|\lambda/\mu|$ . Note that we may view *partition*  $\lambda$  as the *shape*  $\lambda/(0)$

FIGURE 2. Illustration: Ferrers diagram  $F_{\lambda/\mu}$  of the shape  $\lambda/\mu = (8, 5, 5, 4, 2, 2, 2) / (3, 2, 2, 1)$ . The *same* Ferrers diagram would arise for the shapes  $(\lambda + (z)) / (\mu + (z))$  and  $(\lambda + (z^{(7)})) / (\mu + (z^{(7)}))$ , for arbitrary  $z \in \mathbb{Z}$ .



The *Ferrers diagram*  $F_{\lambda/\mu}$  of shape  $\lambda/\mu$  is an array of cells with  $\ell(\lambda/\mu)$  left-justified rows and  $(\lambda_i - \mu_i)$  cells in row  $i$ , where the first  $\mu_i$  cells in row  $i$  are missing, see Figure 2 for an illustration.

Note that for arbitrary  $z \in \mathbb{Z}$ , the Ferrers diagram  $F_{\lambda/\mu}$  also can be written as

$$F_{\lambda/\mu} = F_{\lambda+(z)/\mu+(z)} = F_{\lambda+(z^{(\ell(\lambda/\mu))})/\mu+(z^{(\ell(\lambda/\mu))})}. \quad (1)$$

In particular,  $F_\lambda$  of partition  $\lambda$  may be viewed as the Ferrers diagram  $F_{\lambda+(z^{(\infty)})/(z^{(\infty)})}$  for *arbitrary*  $z \in \mathbb{Z}$ .

*Schur functions*, which are irreducible general linear characters, can be defined as quotient of alternants [14] as follows. Let  $\lambda$  be a partition and let  $\{x_1, \dots, x_n\}$  be a set of independent variables. Then the Schur function  $s_\lambda(x_1, \dots, x_n)$  indexed by  $\lambda$  is defined as the quotient of determinants (see [11, (3.1)])

$$s_\lambda(x_1, \dots, x_n) := \frac{|x_i^{\lambda_j+n-j}|_{i,j=1}^n}{|x_i^{n-j}|_{i,j=1}^n}. \quad (2)$$

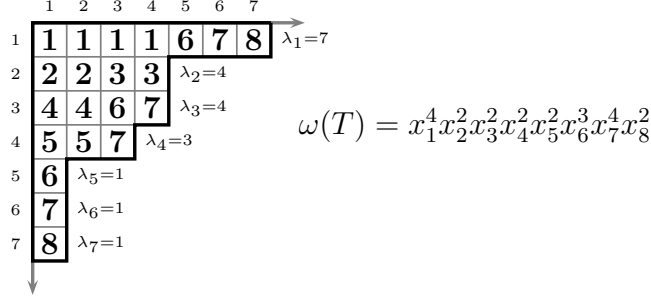
It is easy to see that  $s_\lambda$  is a *symmetric function*, which is homogeneous of degree  $|\lambda|$ . The Jacobi–Trudi identity (first obtained by Jacobi [6] and simplified by Trudi [16], see [11, (3.4)]) states that the Schur function  $s_\lambda$  equals the following determinant of complete homogeneous functions:

$$s_\lambda = |h_{\lambda_j-j+i}|_{i,j=1}^{\ell(\lambda)}. \quad (3)$$

Here, we introduced in passing the shortened notations  $s_\lambda$  and  $h_r$  for  $s_\lambda(x_1, \dots, x_n)$  and  $h_r(x_1, \dots, x_n)$ , respectively.

An *n-semistandard Young tableau* of shape  $\lambda$  is a filling of the cells of the Ferrers diagram  $F_\lambda$  with integers from the set  $\{1, 2, \dots, n\}$ , such that the numbers filled into the cells weakly increase in rows and strictly increase in columns.

FIGURE 3. Illustration: An 8-semistandard Young tableau  $T$  of shape  $\lambda = (7, 4, 4, 3, 1, 1, 1)$  and its weight  $\omega(T)$ .



Let  $T$  be a semistandard Young tableau and define  $\#(T, k)$  to be the number of entries  $k$  in  $T$ . The *weight*  $\omega(T)$  of  $T$  is defined as follows:

$$\omega(T) = \prod_{k=1}^n x_k^{\#(T, k)}. \quad (4)$$

See Figure 3 for an illustration.

Then the *Schur function*  $s_\lambda$  can equivalently be written as the following *generating function* (formal sum of weights)

$$s_\lambda = \sum_T \omega(T),$$

where the sum is over all  $n$ -semistandard Young tableaux  $T$  of shape  $\lambda$  (see [13, Definition 4.4.1]).

An  $n$ -semistandard skew Young tableau of shape  $\lambda/\mu$  is a filling of the cells of  $F_{\lambda/\mu}$  with integers from the set  $\{1, 2, \dots, n\}$ , such that the numbers filled into the cells weakly increase in rows and strictly increase in columns. See the left picture in Figure 5 (or Figure 3 again) for an illustration.

Then we can define the *skew Schur function*  $s_{\lambda/\mu}$  as the following generating function:

$$s_{\lambda/\mu} := \sum_T \omega(T), \quad (5)$$

where the sum is over all  $n$ -semistandard skew Young tableaux  $T$  of shape  $\lambda/\mu$ , where the weight  $\omega(T)$  of  $T$  is defined as in (4).  $s_{\lambda/\mu}$  also is a symmetric function (see [13, proof of Proposition 4.4.2]), which is homogeneous of degree  $|\lambda/\mu|$ . By (1), we clearly have for arbitrary  $z \in \mathbb{Z}$ :

$$s_{\lambda/\mu} = s_{\lambda+(z)/\mu+(z)} = s_{\lambda+(z(\ell(\lambda/\mu)))/\mu+(z(\ell(\lambda/\mu)))}. \quad (6)$$

In particular,  $s_{\lambda+(z(\infty))/(z(\infty))} = s_{\lambda+(z(\ell(\lambda/\mu)))/(z(\ell(\lambda/\mu)))}$  is identical to the “ordinary” Schur function  $s_\lambda$ .

Skew Schur functions, too, have an expansion in terms of complete homogeneous functions (see [11, (5.4)]) which generalizes (3):

$$s_{\lambda/\mu} = \left| h_{\lambda_j - \mu_i - j + i} \right|_{i,j=1}^{\ell(\lambda)}. \quad (7)$$

**2.3. Connection between determinantal relations and Schur function identities.** We want to illustrate the connection between determinants and skew Schur functions, using Dodgson's condensation formula as an example.

Consider some  $m \times n$ -matrix  $a = (a_{i,j})_{(i,j)=(1,1)}^{(m,n)}$  and define  $[k] := \{1, 2, \dots, k\}$  for  $k \in \mathbb{N}$ . Then we may write  $a = (a)_{[m], [n]} := (a_{i,j})_{(i,j) \in [m] \times [n]}$ . More generally, for subsets  $R \subseteq [m]$  and  $C \subseteq [n]$ , we denote by  $(a)_{R, C}$  the *minor* of  $a$  which consists of the rows  $R$  and the columns  $C$ ; *in the same order as in  $a$* . (All sets we consider in this paper are *ordered*, and all subsets “inherit the order”.)

If we want to describe the same minor by deleting rows and columns in  $a$ , then we write

$$(a)_{R, C} = (a)_{\overline{X}, \overline{Y}},$$

where  $X = \overline{R} := [m] \setminus R$  and  $Y = \overline{C} := [n] \setminus C$ .

**Proposition 2** (Dodgson's Condensation). *Let  $a = (a_{i,j})_{i,j=1}^m$  be an arbitrary  $m \times m$ -matrix,  $m \geq 2$ . Then there holds the following identity:*

$$|a| \cdot \left| (a)_{\overline{\{1,m\}}, \overline{\{1,m\}}} \right| = \left| (a)_{\overline{\{1\}}, \overline{\{1\}}} \right| \cdot \left| (a)_{\overline{\{m\}}, \overline{\{m\}}} \right| - \left| (a)_{\overline{\{1\}}, \overline{\{m\}}} \right| \cdot \left| (a)_{\overline{\{m\}}, \overline{\{1\}}} \right|. \quad (8)$$

(Note that for  $m = 2$ , this amounts to the formula for  $2 \times 2$ -determinants.)  $\square$

We shall “translate” this determinantal identity to a Schur function identity. To this end, we introduce the following operation “delete part  $\lambda_k$  in semipartition  $\lambda$ ”:

$$\lambda^{\overline{k}} := (\lambda_1, \dots, \lambda_{k-1}, \lambda_{k+1} - 1, \lambda_{k+2} - 1, \dots). \quad (9)$$

Note that  $\lambda_{\infty}^{\overline{k}} = \lambda_{\infty} - 1$  and  $\ell(\lambda^{\overline{k}}) = \max(\ell(\lambda), k) - 1$ .

For some subset  $\{k_1 < k_2 < \dots < k_l\} \subseteq \{1, 2, \dots, m\}$ , we define inductively:

$$\lambda^{\overline{k_1, \dots, k_l}} := \left( \lambda^{\overline{k_2, \dots, k_l}} \right)^{\overline{k_1}}.$$

Now assume some skew shape  $\lambda/\mu$ ,  $m = \ell(\lambda/\mu)$ . According to (7), the skew Schur function  $s_{\lambda/\mu}$  equals the determinant of the matrix

$$\mathbf{h}_{\lambda/\mu} := \left( h_{\lambda_j - \mu_i - j + i} \right)_{(i,j)=1,1}^{(m,m)}.$$

Observe that the  $(i, j)$ -entries in matrix  $(\mathbf{h}_{\lambda/\mu})_{\overline{\emptyset}, \overline{\{k\}}}$  are

- $h_{\lambda_j - \mu_i - j + i}$  for  $j < k$ ,
- $h_{(\lambda_{j+1}-1) - \mu_i - j + i}$  for  $k \leq j \leq m - 1$

(i.e., deleting column  $k$  in  $\mathbf{h}_{\lambda/\mu}$  corresponds to deleting  $\lambda_k$  in  $\lambda$ ), while the  $(i, j)$ -entries in matrix  $(a_{\lambda/\mu})_{\overline{\{l\}}, \overline{\emptyset}}$  are

- $h_{\lambda_j - \mu_i - j + i}$  for  $i < l$ ,
- $h_{\lambda_j - (\mu_{i+1} - 1) - j + i}$  for  $l \leq i \leq m - 1$

(i.e., deleting row  $l$  in  $\mathbf{h}_{\lambda/\mu}$  corresponds to deleting  $\mu_l$  in  $\mu$ ). These observations generalize to the following relation:

$$(\mathbf{h}_{\lambda/\mu})_{\overline{\{i_1, \dots, i_k\}}, \overline{\{j_1, \dots, j_l\}}} = \mathbf{h}_{\lambda_{\overline{i_1, \dots, i_k}}/\mu_{\overline{j_1, \dots, j_l}}}. \quad (10)$$

So we can deduce the following Schur function identity:

**Corollary 1.** *Let  $\lambda = (\lambda_1, \lambda_2, \dots, \lambda_m)$  be a partition of length  $\ell(\lambda) = m \leq 2$ . Then we have the following Schur function identity:*

$$s_\lambda \cdot s_{(\lambda_2, \lambda_3, \dots, \lambda_{m-1})} = s_{(\lambda_2, \lambda_3, \dots, \lambda_m)} \cdot s_{(\lambda_1, \lambda_2, \dots, \lambda_{m-1})} - s_{(\lambda_2 - 1, \lambda_3 - 1, \dots, \lambda_m - 1)} \cdot s_{(\lambda_1 + 1, \lambda_2 + 1, \dots, \lambda_{m-1} + 1)} \quad (11)$$

To provide a combinatorial proof for (a special case of) this identity was the initial point for the work in [2].

*Proof.* Consider the matrix  $\mathbf{h}_{(\lambda + (1^{(m)})) / (1^{(m)})}$  (which is equal to  $\mathbf{h}_\lambda$ ). Then (8) translates to

$$s_{(\lambda + (1^{(m)})) / (1^{(m)})} \cdot s_{(\lambda + (1^{(m)}))^{1, \overline{m}} / (1^{(m)})^{1, \overline{m}}} = s_{(\lambda + (1^{(m)}))^{1, \overline{m}} / (1^{(m)})^{1, \overline{m}}} \cdot s_{(\lambda + (1^{(m)}))^{1, \overline{m}} / (1^{(m)})^{1, \overline{m}}} - s_{(\lambda + (1^{(m)}))^{1, \overline{m}} / (1^{(m)})^{1, \overline{m}}} \cdot s_{(\lambda + (1^{(m)}))^{1, \overline{m}} / (1^{(m)})^{1, \overline{m}}}.$$

by (7) and (10). By (6) this simplifies to

$$s_\lambda \cdot s_{(\lambda + (1^{(m)}))^{1, \overline{m}}} = s_{(\lambda + (1^{(m)}))^{1, \overline{m}}} \cdot s_{(\lambda)^{\overline{m}}} - s_{(\lambda)^{\overline{m}}} \cdot s_{(\lambda + (1^{(m)}))^{1, \overline{m}}},$$

which is equivalent to (11).  $\square$

So far, we proved the Schur function identity (11) by recognizing it as a special case of the general determinantal identity (8). But this works also the other way round:

**Observation 1** (Schur function identities imply equivalent determinantal identities). *Assume that we have an identity  $\mathcal{S}$  involving skew Schur functions.*

*Then by (7) and Proposition 1,  $\mathcal{S}$  translates to a determinantal identity  $\mathcal{D}$  which is equivalent to  $\mathcal{S}$  as follows:*

- Rewrite each skew Schur function in  $\mathcal{S}$  as a determinant of complete homogeneous functions, according to (7),
- and then replace each entry  $h_r$  by variable  $y_r$ , where  $(y_r)_{r=0}^\infty$  is a set of independent variables, according to Proposition 1.

We call (skew) Schur function identities which are valid for *arbitrary* shapes  $\lambda/\mu$  *generic* (skew) Schur function identities: Note that (11) is a generic identity in this sense. All identities we shall consider in the rest of this paper are generic.

In particular, we may apply (11) to  $\lambda = (\lambda_1, \dots, \lambda_m)$ , where  $\lambda_j = (m - j + 1) \cdot (m)$ . It is easy to see that for this choice of  $\lambda$ , all the entries in  $(h_{\lambda_j - j + i})_{i,j=1}^m$  are *distinct*,

whence we may replace them by independent variables (by Proposition 1). This means that (11) implies the *general* determinantal identity (8): The identities are, in fact, *equivalent*.

It is clear, that this phenomenon will apply also to other determinantal identities: In this paper, we shall present *generic* Schur function identities which are equivalent to classical determinantal identities, and give combinatorial proofs for these Schur function identities.

### 3. DETERMINANTS AS NONINTERSECTING LATTICE PATHS

The Lindström–Gessel–Viennot–method [3, 10, 7] is well-known: But since we want to present a “nonintersecting lattice path”–proof of the Cauchy–Binet formula (19) which involves a slight generalization, we repeat this beautiful idea here in some detail, using the Jacobi–Trudi–determinant as an illustrating example.

**3.1. Lattice paths.** Consider the square lattice  $\mathbb{Z}^2$ , i.e., the directed graph with vertices  $\mathbb{Z} \times \mathbb{Z}$  (we shall call them *points*), where the set of arcs consists of

- horizontal arcs  $a_{(j,k)}^h$  from  $(j, k)$  to  $(j + 1, k)$  for  $j, k \in \mathbb{Z}$ , and
- vertical arcs  $a_{(j,k)}^v$  from  $(j, k)$  to  $(j, k + 1)$  for  $j, k \in \mathbb{Z}$ .

Assign to these arcs the following weights:

$$\begin{aligned}\omega(a_{(j,k)}^v) &:= 1 \text{ (i.e., vertical arcs have weight 1),} \\ \omega(a_{(j,k)}^h) &:= x_k \text{ (i.e., horizontal arcs have weight } x_{\text{height of the arc}}\text{).}\end{aligned}$$

A *lattice path*  $p$  of length  $k$  connecting starting point  $v$  to ending point  $w$  is a sequence of points  $(v = v_0, v_1, \dots, v_k = w)$ , such that  $(v_{i-1}, v_i)$  is a (horizontal or vertical) arc  $a_i$  for  $i = 1, 2, \dots, k$ . We say that all these arcs  $a_i$  and points  $v_i$  *belong* to the path  $p$  and write  $a_i \in p$  and  $v_i \in p$ .

For some set  $S$  of points (arcs) we denote by  $p \cap S$  the set of points (arcs) in  $S$  that belong to  $p$ . The weight of  $p$  is defined as the product of the weights of the arcs belonging to  $p$

$$\omega(p) = \prod_{a \in p} \omega(a). \quad (12)$$

Denote by  $\mathfrak{P}(v \rightarrow w)$  the set of *all* lattice paths connecting starting point  $v$  to ending point  $w$ . Observe that we may view the complete homogeneous symmetric function

$$h_m(x_j, x_{j+1}, \dots, x_k), k \geq j$$

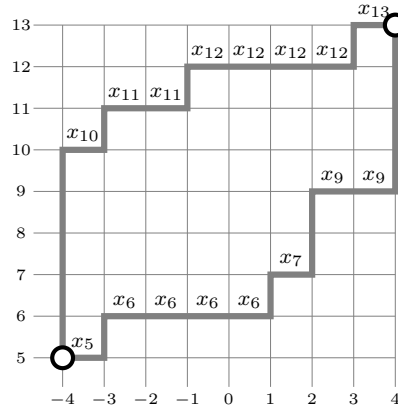
as the *generating function* of  $\mathfrak{P}(v \rightarrow w)$ , where  $v = (t, j)$  and  $w = (t + m, k)$ , with arbitrary  $t \in \mathbb{Z}$ :

$$\mathbf{gf}(\mathfrak{P}(v \rightarrow w)) = \sum_p \omega(p),$$

where the sum is over all paths  $p$  connecting  $v$  and  $w$ . (See Figure 4.)



FIGURE 4. Complete homogeneous symmetric functions may be viewed as generating functions of lattice paths with fixed starting (lower) and ending (upper) point. The picture below illustrates this for  $h_8(x_5, x_6, \dots, x_{13})$ , which appears as the sum of the weights of all lattice paths connecting starting point  $(-4, 5)$  to ending point  $(4, 13)$ , showing the lattice paths associated to the two monomials  $(x_5 \cdot x_6^4 \cdot x_7 \cdot x_9^2)$  and  $(x_{10} \cdot x_{11}^2 \cdot x_{12}^4 \cdot x_{13})$  in  $h_8(x_5, x_6, \dots, x_{13})$ . Note that we may shift the picture horizontally by an arbitrary vector  $(t, 0)$ ,  $t \in \mathbb{Z}$ , without changing the generating function of the lattice paths.



Note that the ending point of some path  $p$  never lies below its starting point. Later, we shall also consider *trails* in the *undirected* graph  $\mathbb{Z}^2$ : A *trail*  $p'$  of length  $k$  connecting point  $v$  to point  $w$  is a sequence of points  $(v = v_0, v_1, \dots, v_k = w)$ , such that  $(v_{i-1}, v_i)$  or  $(v_i, v_{i-1})$  is a (horizontal or vertical) arc  $a_i$  for  $i = 1, 2, \dots, k$  (i.e.,  $p'$  may use arcs “in the wrong direction”). For such trail, it is not clear whether  $v$  or  $w$  is the starting or ending point, so in order to avoid confusion, for some lattice path  $p$  we shall call

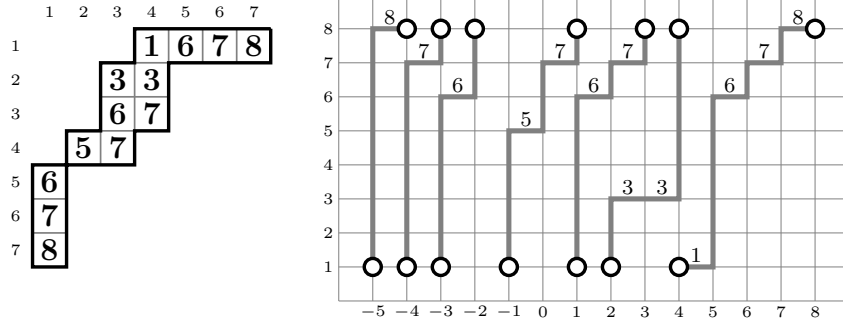
- the starting point  $p$  its *lower* point,
- and the ending point  $p$  its *upper* point

from now on.

**3.2. Young tableaux and nonintersecting lattice paths.** The Lindström–Gessel–Viennot interpretation gives an equivalent description of a semistandard Young tableau  $T$  of shape  $\lambda/\mu$  as an  $m$ -tuple  $P = (p_1, \dots, p_m)$  of nonintersecting lattice paths, where  $m := \ell(\lambda/\mu)$ , as follows. The  $i$ -th path  $p_i$  starts at lower point  $(\mu_i - i, 1)$  and ends at upper point  $(\lambda_i - i, n)$ : We call these points the lower/upper points associated to the skew shape  $\lambda/\mu$ , and we count these points always *from the right*. The  $k$ -th *horizontal* step in  $p_i$  goes from  $(\mu_i - i + k - 1, x)$  to  $(\mu_i - i + k, x)$ , where  $x$  is the  $k$ -th entry in row  $i$  of  $T$ .

Note that the conditions on the entries of  $T$  imply that no two paths  $p_i$  and  $p_j$  thus defined have a lattice point in common: Such an  $m$ -tuple of paths is called *nonintersecting*, see the right picture of Figure 5 for an illustration. An  $m$ -tuple of paths which is *not* nonintersecting is called *intersecting*.

FIGURE 5. The left picture presents a semistandard Young tableau  $T$  of shape  $\lambda/\mu$ , where  $\lambda = (9, 6, 6, 5, 3, 3, 3)$  and  $\mu = (5, 4, 4, 3, 2, 2, 2)$ . Assuming that the entries of  $T$  are chosen from  $\{1, 2, \dots, 8\}$  (i.e.:  $T$  is an 8-semistandard Young tableau), the right picture shows the corresponding family of  $7 = \ell(\lambda/\mu)$  nonintersecting lattice paths: Note that the height of the  $j$ -th horizontal step in the  $i$ -th path (the paths are counted from right to left) is equal to the  $j$ -th entry in row  $i$  of  $T$ .



In fact, this translation of tableaux to nonintersecting lattice paths is a *bijection* between the set of all  $n$ -semistandard Young tableaux of shape  $\lambda/\mu$  and the set of all  $\ell(\lambda/\mu)$ -tuples of nonintersecting lattice paths with lower (starting) and upper (ending) points as defined above.

This bijection is *weight preserving* if we define the weight of an  $m$ -tuple  $P = (p_1, \dots, p_m)$  of lattice paths in the obvious way, i.e., as

$$\omega(P) := \prod_{k=1}^m \omega(p_k) = \prod_{k=1}^n x_k^{\#(P,k)}, \quad (13)$$

where  $\#(P, k)$  is the number of horizontal steps at height  $k$  in  $P$ . So in definition (5) we could equivalently replace symbol “ $T$ ” by symbol “ $P$ ”, and sum over  $m$ -tuples of nonintersecting lattice paths with prescribed lower and upper points instead of tableaux with prescribed shape.

Note that the horizontal coordinates of lower and upper points determine uniquely the *shape*  $\lambda/\mu$  of the tableau, and the vertical coordinate (we shall call the vertical coordinate of points the *level* in the following) of the ending points determines uniquely the *set of entries*  $\{1, 2, \dots, n\}$  of the tableau. (The choice of the shift parameter  $t$  does influence neither the shape nor the set of entries.)

Observe that the operation of deleting part  $i$  in  $\mu = (\mu_1, \dots, \mu_m)$  and part  $j$  in  $\lambda = (\lambda_1, \dots, \lambda_m)$  (defined in (9)) translates to the removal of the  $i$ -th lower point and the  $j$ -th upper point associated to  $\lambda/\mu$ , and by (10), this removal of lower/upper points translates to deleting row  $i$  and column  $j$  in  $\mathbf{h}_{\lambda/\mu}$ . Clearly, this generalizes to the following observation:

**Observation 2.** *Minors of  $\mathbf{h}_{\lambda/\mu}$  consisting of rows  $\{i_1, \dots, i_k\}$  and columns  $\{j_1, \dots, j_l\}$  are in one-to-one correspondence to the selection of*

- lower points with indices in  $\{i_1, \dots, i_k\}$

- and upper points with indices in  $\{j_1, \dots, j_l\}$

from the points associated to the shape  $\lambda/\mu$ .

**3.3. The Lindström–Gessel–Viennot–proof of the Jacobi–Trudi identity.** Denote the  $i$ -th lower point  $(\mu_i - i, 1)$  by  $s_i$ , and the  $j$ -th ending point  $(\lambda_j - j, n)$  by  $t_j$ . Observe that the entry  $(i, j)$  in the matrix  $\mathbf{h}_{\lambda/\mu}$  is the *generating function*

$$\mathbf{gf}(\mathfrak{P}(s_i \rightarrow t_j)) := \sum_p \omega(p) = h_{\lambda_j - \mu_i - j + i},$$

where the sum is over all lattice paths  $p$  that run from  $s_i$  to  $t_j$ , and where the weight  $\omega(p)$  is defined as in (12). By expanding the determinant in (7), we thus obtain

$$\left| h_{\lambda_j - \mu_i - j + i} \right|_{i,j=1}^m = \sum_{\pi \in \mathfrak{S}_m} \text{sgn}(\pi) \cdot \prod_{j=1}^m (\mathbf{gf}(\mathfrak{P}(s_{\pi_j} \rightarrow t_j))), \quad (14)$$

where  $m = \ell(\lambda/\mu)$ . Consider the following set

$$\mathfrak{D}_{\lambda/\mu} := \bigcup_{\pi \in \mathfrak{S}_m} \mathfrak{P}(s_{\pi_1} \rightarrow t_1) \times \mathfrak{P}(s_{\pi_2} \rightarrow t_2) \times \dots \times \mathfrak{P}(s_{\pi_m} \rightarrow t_m)$$

of  $m$ -tuples  $P$  of lattice paths connecting the permuted lower points  $(s_{\pi_1}, s_{\pi_2}, \dots, s_{\pi_m})$  with the upper points  $(t_1, t_2, \dots, t_m)$ , where in addition to the weight  $\omega(P)$ , the elements of  $\mathfrak{D}_{\lambda/\mu}$  also carry a *sign* which equals the sign of the respective permutation  $\pi$ :

$$\text{sgn}(P) = \text{sgn}(\pi).$$

Then (14) can be rewritten equivalently as the generating function of  $\mathfrak{D}_{\lambda/\mu}$ :

$$\left| h_{\lambda_j - \mu_i - j + i} \right|_{i,j=1}^m = \sum_{P \in \mathfrak{D}_{\lambda/\mu}} \text{sgn}(P) \cdot \omega(P). \quad (15)$$

Denote by  $\mathfrak{N}_{\lambda/\mu}$  the subset of *nonintersecting*  $m$ -tuples of lattice paths in  $\mathfrak{D}_{\lambda/\mu}$ . In order to prove (7), we only need to show that we do in fact have

$$\left| h_{\lambda_j - \mu_i - j + i} \right|_{i,j=1}^m = \sum_{P \in \mathfrak{N}_{\lambda/\mu}} \text{sgn}(P) \cdot \omega(P), \quad (16)$$

since  $P \in \mathfrak{N}_{\lambda/\mu}$  implies  $\pi = \text{id}$  (i.e., all these “surviving” objects have sign +1) and  $s_{\lambda/\mu} = \sum_{P \in \mathfrak{N}_{\lambda/\mu}} \text{sgn}(P) \cdot \omega(P)$  by definition (5). This certainly can be achieved by showing that all the signed weights of  $m$ -tuples  $P$  in  $\mathfrak{J}_{\lambda/\mu} := \mathfrak{D}_{\lambda/\mu} \setminus \mathfrak{N}_{\lambda/\mu}$  *cancel* in (15). To this end, we shall present an *involution* (a self-inverse bijective mapping) on *intersecting*  $m$ -tuples of lattice paths

$$\mathbf{i}: (\mathfrak{J}_{\lambda/\mu}) \rightarrow (\mathfrak{J}_{\lambda/\mu})$$

which is

- *weight-preserving*, i.e.,  $\omega(\mathbf{i}(P)) = \omega(P)$
- and *sign-reversing*, i.e.,  $\text{sgn}(\mathbf{i}(P)) = -\text{sgn}(P)$ .

The construction of  $\mathbf{i}$  is simple: Let  $P$  be an *intersecting*  $m$ -tuple in  $\mathfrak{J}_{\lambda/\mu}$ . Consider the *smallest* point of intersection  $q$  in  $P$ , in lexicographic order:

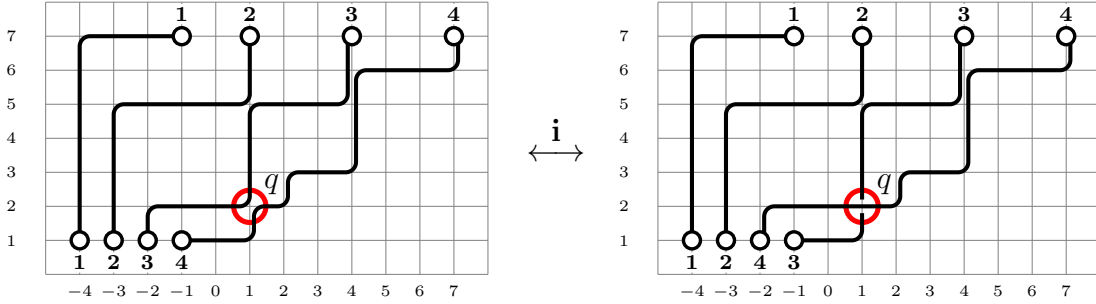
$$(a, b) \leq (c, d) :\Leftrightarrow a \leq b \vee (a = b \wedge b \leq c).$$

FIGURE 6. Illustration of the Lindström–Gessel–Viennot–involution  $\mathbf{i}$ . Both pictures show quadruples of lattice paths belonging to  $\mathfrak{J}_{\lambda/\mu}$ , where  $\lambda = (8, 6, 4, 3)$  and  $\mu = (0)$ . There are 4 points of intersections at positions

$$(6, 2) < (6, 5) < (9, 5) < (9, 6),$$

written in lexicographic order. (Note that the lattice paths are drawn with rounded corners and small offsets here, just to make obvious the run of the paths, which is not clear for intersecting paths). The smallest such point in lexicographic order is  $q := (6, 2)$  (indicated by a circle). The right picture is obtained from the left picture by interchanging the initial segments (from lower points up to  $q$ ) of the two paths intersecting in  $q$ , and vice versa. To the left picture, the identity permutation (i.e., sign +1) is associated, while to the right picture, the transposition  $(3, 4)$  (i.e., sign  $-1$ ) is associated. This illustrates that in the determinantal expansion of  $s_\lambda = |h_{\lambda_j - j + i}|$ , the following terms cancel:

$$(x_7^3)(x_5^4)(x_2^3x_5^3)(x_1^2x_2x_3^2x_6^3) - (x_7^3)(x_5^4)(x_2^4x_3^2x_6^3)(x_1^2x_5^3) = 0.$$



Observe that there are precisely *two* paths  $p_k$  and  $p_l$  meeting in  $q$  (by the minimality of  $q$ ):  $\mathbf{i}(P)$  is obtained from  $P$  by *interchanging* the initial segments (from lower points up to  $q$ ) of  $p_k$  and  $p_l$ , see Figure 6 for an illustration.

It is immediately clear that  $\mathbf{i}$  is an involution which is weight-preserving and sign-reversing (since it modifies the original permutation associated to  $P$  by the transposition corresponding to the swapping of the lower points of  $p_k$  and  $p_l$ ).

Clearly,  $\mathbf{i}$  describes the pairwise cancellation

$$\text{sgn}(P) \cdot \omega(P) + \mathbf{i}(\text{sgn}(P) \cdot \omega(P)) = 0$$

of all objects from  $\mathfrak{J}_{\lambda/\mu}$  in the sum (15). Stated otherwise: Only the *nonintersecting* objects in  $\mathfrak{N}_{\lambda/\mu} \subseteq \mathfrak{D}_{\lambda/\mu}$  “survive”, which proves (16).  $\square$

**3.4. Viewing determinants as nonintersecting lattice paths.** Our considerations so far showed that the *generic* determinant  $(y_{i,j})_{i,j=1}^m$  (here, generic means that the entries are independent variables) may be viewed as a skew Schur function of *appropriate* shape  $\lambda/\mu$  (here, appropriate means all entries in  $\mathbf{h}_{\lambda/\mu}$  are distinct), hence as the *generating function of nonintersecting lattice paths*.

We shall demonstrate the power of this point of view by giving a simple proof of the Cauchy–Binet formula (19), which will become even more transparent if we prove the multiplicativity of the determinant function as a preparatory step.

3.4.1. *Multiplicativity of the determinant function: A proof “by example”.* Given some arc  $a$  in the lattice  $\mathbb{Z}^2$ , we say that a path  $p$  *starts* in  $a$  (has  $a$  as its *lower* arc), if  $p$  starts in the upper (if  $a$  is vertical) or right (if  $a$  is horizontal) point of  $a$ . Likewise, we say that  $p$  *ends* in  $a$  (has  $a$  as its *upper* arc), if  $p$  ends in the lower (if  $a$  is vertical) or left (if  $a$  is horizontal) point of  $a$ .

We want to illustrate the multiplicativity of the determinant function

$$|a \cdot b| = |a| \cdot |b| \quad (17)$$

by considering the special case

$$a := \left( h_{\lambda_j - j + i}(x_1, x_2, \dots, x_7) \right)_{i,j=1}^4 \quad \text{and} \quad b := \left( h_{\sigma_j - \lambda_i - j + i}(x_8, x_9, \dots, x_{13}) \right)_{i,j=1}^4,$$

where  $\lambda = (8, 6, 4, 3)$  and  $\sigma = (18, 16, 13, 11)$ .

By the Lindström–Gessel–Viennot–interpretation, we may view  $|a|$  as the generating function of quadruples of nonintersecting lattice paths connecting lower points  $\mathbf{r} = (r_1, r_2, r_3, r_4)$  with upper arcs  $\mathbf{s} = (s_1, s_2, s_3, s_4)$ , where

$$\begin{aligned} \mathbf{r} &= ((-1, 1), (-2, 1), (-3, 1), (-4, 1)), \\ \mathbf{s} &= (((7, 7), (7, 8)), ((4, 7), (4, 8)), ((1, 7), (1, 8)), ((-1, 7), (-1, 8))). \end{aligned}$$

Likewise, we may view  $|b|$  as the generating function of quadruples of nonintersecting lattice paths connecting lower arcs  $\mathbf{s}$  (as above: Note that the set of variables involved in  $b$  is  $\{x_8, \dots, x_{13}\}$ !) with ending points  $\mathbf{t} = (t_1, t_2, t_3, t_4)$ , where

$$\mathbf{t} = ((17, 13), (14, 13), (10, 13), (7, 13)).$$

See Figure 7 for an illustration.

So the  $(i, j)$ –entry in  $a \cdot b$  is

$$\sum_{k=1}^4 \mathbf{gf}(\mathfrak{P}(r_i \rightarrow s_k)) \cdot \mathbf{gf}(\mathfrak{P}(s_k \rightarrow t_j)),$$

which may be viewed as the generating function  $\mathbf{gf}(\mathfrak{P}'(r_i \rightarrow t_j))$  of the following set of *constrained* paths (see Figure 8 for an illustration):

$$\mathfrak{P}'(r_i \rightarrow t_j) := \bigcup_{k=1}^4 \{p : p \text{ is a lattice path connecting } r_i \text{ to } t_j \text{ passing through } s_k\}.$$

So as in the above proof of the Jacobi–Trudi identity,  $|a \cdot b|$  can be rewritten equivalently as the generating function of the set  $\mathfrak{D}'$  of quadruples of *constrained* paths,

$$\mathfrak{D}' := \bigcup_{\pi \in \mathfrak{S}_4} \mathfrak{P}'(s_{\pi_1} \rightarrow t_1) \times \mathfrak{P}'(s_{\pi_2} \rightarrow t_2) \times \mathfrak{P}'(s_{\pi_3} \rightarrow t_3) \times \mathfrak{P}'(s_{\pi_4} \rightarrow t_4),$$

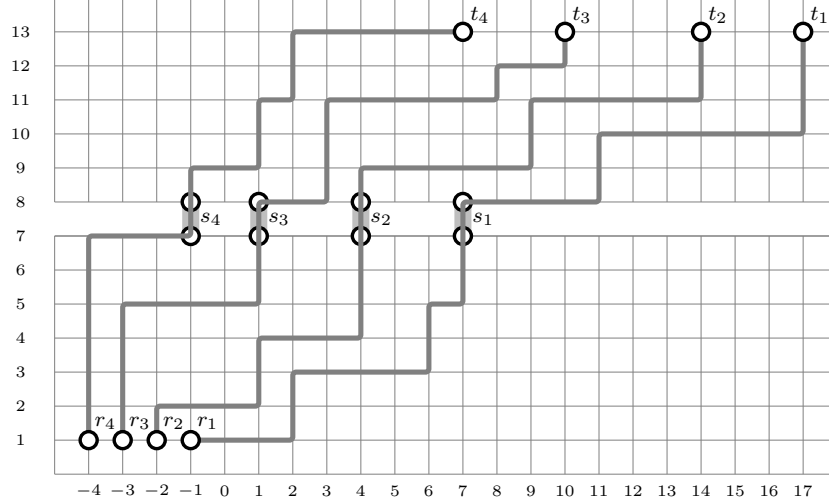
FIGURE 7. Illustration: Multiplicativity of the determinant. The picture shows the lattice paths corresponding to the monomial

$$((x_7^3) \cdot (x_9^2 x_{11} x_{13}^5)) \cdot ((x_5^4) \cdot (x_7^2 x_{11}^5 x_{12}^2)) \cdot ((x_2^3 x_4^3) \cdot (x_9^5 x_{11}^5)) \cdot ((x_1^3 x_3^4 x_5) \cdot (x_8^4 x_{10}^6)),$$

which appears in the expansion of the product of skew Schur functions

$$s_\lambda(x_1, x_2, \dots, x_7) \cdot s_{\sigma/\lambda}(x_8, x_9, \dots, x_{13}),$$

where  $\lambda = (8, 6, 4, 3)$  and  $\sigma = (18, 16, 13, 11)$ .



i.e., as

$$|a \cdot b| = \sum_{P \in \mathfrak{D}'} \text{sgn}(P) \cdot \omega(P). \quad (18)$$

Denote by  $\mathfrak{N}'$  the subset of *nonintersecting*  $m$ -tuples of constrained lattice paths in  $\mathfrak{D}'$ . Clearly, the Lindström–Gessel–Viennot–operation  $\mathbf{i}$  can be applied to *intersecting*  $m$ -tuples of constrained lattice paths (see Figure 8 for an illustration) and establishes a weight–preserving and sign–reversing involution, i.e.,

$$|a \cdot b| = \mathbf{gf}(\mathfrak{N}').$$

On the other hand,  $\mathfrak{N}'$  appears (just *look* at Figure 7!) as the Cartesian product of

- the set of nonintersecting quadrupels of lattice paths connecting  $\mathbf{r}$  and  $\mathbf{s}$
- and the set of nonintersecting quadrupels of lattice paths connecting  $\mathbf{s}$  and  $\mathbf{t}$ ,

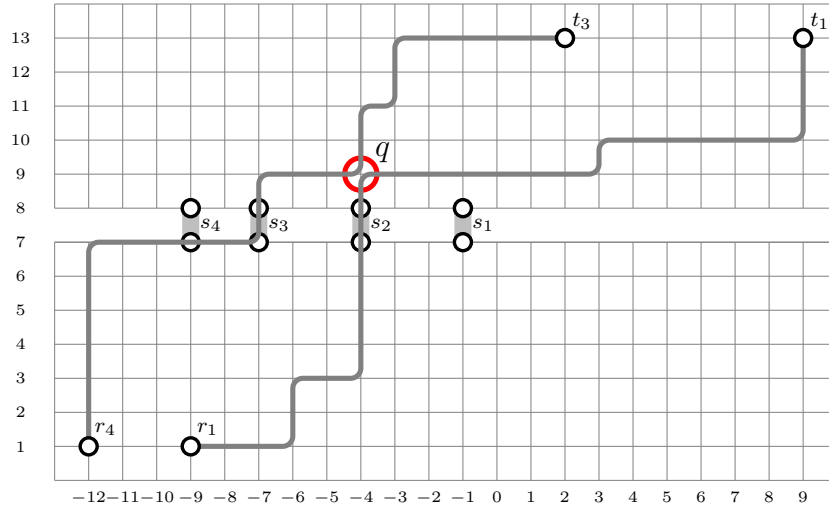
i.e.,

$$\mathbf{gf}(\mathfrak{N}') = |a| \cdot |b|.$$

We presented our argument for a specific choice of partitions  $\lambda \leq \sigma$  to make it more tangible, but it is clear that it holds for arbitrary choices of (semi)partitions. So fix  $m > 0$  and consider the following partitions  $\lambda$  and  $\sigma$ ,  $\ell(\lambda) = \ell(\sigma) = m$ :

$$\begin{aligned} \lambda &= ((m \cdot (m-1), (m-1) \cdot (m-1), \dots, (m-1)) \text{ (i.e., } \lambda_j = (m-j+1) \cdot (m-1)), \\ \sigma &= \left( (m \cdot m)^{(m)} \right) = (m^2, m^2, \dots, m^2) \text{ (i.e., } \sigma_i = m^2). \end{aligned}$$

FIGURE 8. Illustration: The Lindström–Gessel–Viennot–involution for the “constrained” lattice paths  $\mathbf{gf}(\mathfrak{P}'(r_i \rightarrow t_j))$ : The fact that *every* constrained path must pass through one of the arcs  $s_1, s_2, s_3$  or  $s_4$  is indicated by omitting all *other* arcs connecting level 7 and level 8. The picture shows a path connecting  $r_1$  to  $t_1$  which passes through the arc  $s_2$ , and a path connecting  $r_4$  to  $t_3$ , which passes through the arc  $s_3$ . The smallest point of intersection in lexicographic order is  $q := (-4, 9)$  (indicated by a circle; as in Figure 6, the lattice paths are drawn with rounded corners here, just to make obvious the run of the paths.) Clearly, the Lindström–Gessel–Viennot–involution gives a path connecting  $r_1$  to  $t_3$  which passes through  $s_2$ , and a path connecting  $r_4$  to  $t_1$  which passes through  $s_3$ .



Then the entries in  $a := \mathbf{h}_\lambda(x_1, \dots, x_n)$  and in  $b := \mathbf{h}_{\sigma/\lambda}(x_{n+1}, \dots, x_{2n})$  are all distinct. Hence (recall Observation 1) the identity

$$|a \cdot b| = |a| \cdot |b|$$

implies the multiplicativity of the determinant function *in general*.  $\square$

3.4.2. *The Cauchy–Binet formula: Another proof “by example”.* Now it is “almost immediate” to see the Cauchy–Binet formula as an obvious generalization of the multiplicativity of the determinant.

**Theorem 1** (Cauchy–Binet formula). *Let  $a$  be an  $m \times n$ -matrix and  $b$  be an  $n \times m$ -matrix. Then we have*

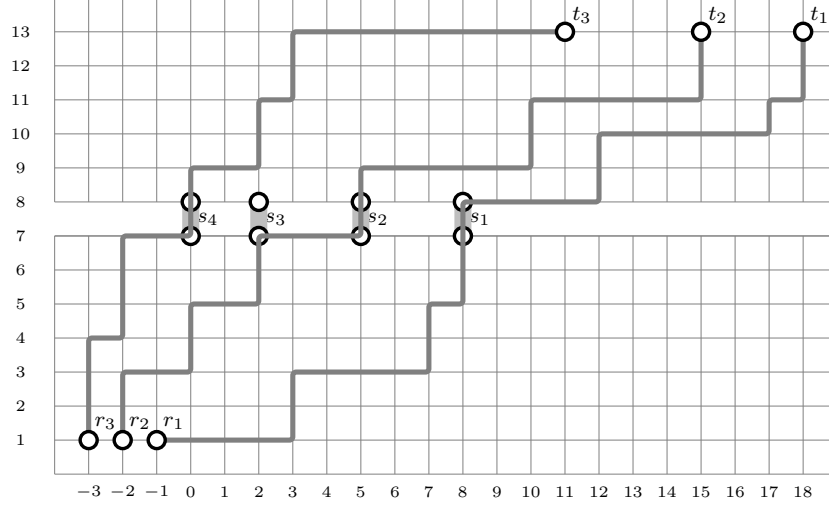
$$|a \cdot b| = \sum_{S \subseteq [n], |S|=m} \left| (a)_{[m], S} \right| \cdot \left| (b)_{S, [m]} \right|. \quad (19)$$

Note that this formula holds trivially if  $m > n$  (since the determinant  $|a \cdot b|$  is zero in this case, as is the empty sum in (19)), and amounts to the multiplicativity of the determinant if  $m = n$ .

We illustrate this formula by a special case and consider the matrices

$$a := \left( h_{\lambda_j - j + i}(x_1, \dots, x_7) \right)_{(i,j) \in ([3] \times [4])} \quad \text{and} \quad b := \left( h_{\sigma_j - \lambda_i - j + i}(x_8, \dots, x_{13}) \right)_{(i,j) \in ([4] \times [3])},$$

FIGURE 9. Illustration: The Cauchy–Binet formula. Triples of nonintersecting lattice paths connecting points  $\mathbf{r} = (r_1, r_2, r_3)$  and  $\mathbf{t} = (t_1, t_2, t_3)$ , where each single path must pass through an arc in  $\mathbf{s} = (s_1, s_2, s_3, s_4)$ , can be “cut in two halves” along  $\mathbf{s}$ . Note that the arcs used by the paths constitute a 3–element subvector  $\mathbf{s}'$ , and the halves appear as tripels of nonintersecting lattice paths  $\mathfrak{N}(\mathbf{r} \rightarrow \mathbf{s}')$  and  $\mathfrak{N}(\mathbf{s}' \rightarrow \mathbf{t})$ , respectively. In the picture, we have  $\mathbf{s}' = (s_1, s_2, s_4)$ .



where  $\lambda = (9, 7, 5, 4)$  and  $\sigma = (19, 17, 14)$ .

Again, we want to employ the Lindström–Gessel–Viennot–interpretation. To this end, we consider the vectors of points  $\mathbf{r} = (r_1, r_2, r_3)$  and  $\mathbf{t} = (t_1, t_2, t_3)$ , and the vector of arcs,  $\mathbf{s} = (s_1, s_2, s_3, s_4)$ , where

$$\begin{aligned} \mathbf{r} &= ((-1, 1), (-2, 1), (-3, 1)), \\ \mathbf{s} &= (((8, 7), (8, 8)), ((5, 7), (5, 8)), ((2, 7), (2, 8)), ((0, 7), (0, 8))), \\ \mathbf{t} &= ((18, 13), (15, 13), (11, 13)), \end{aligned}$$

(See Figure 9 for an illustration.)

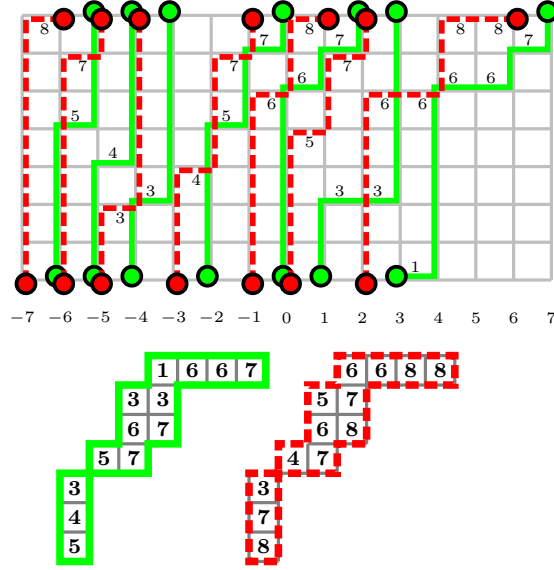
As before, observe that the  $(i, j)$ –entry in  $a \cdot b$  may be viewed as the generating function  $\mathbf{gf}(\mathfrak{P}(r_i \rightarrow t_j))'$  of *constrained* paths which must pass through one arc in  $\mathbf{s}$ . By the Lindström–Gessel–Viennot–involution, the determinant  $|a \cdot b|$  appears as the generating function of quadrupels of nonintersecting labeled paths  $\mathfrak{N}'(\mathbf{r} \rightarrow \mathbf{t})$ , which (as above — just *look* at Figure 9!) appears as

$$\mathfrak{N}'(\mathbf{r} \rightarrow \mathbf{t}) = \bigcup_{\mathbf{s}'} (\mathfrak{N}(\mathbf{r} \rightarrow \mathbf{s}') \times \mathfrak{N}(\mathbf{s}' \rightarrow \mathbf{t}),)$$

where the union runs over all 3–element subvectors  $\mathbf{s}'$  of  $\mathbf{s}$ . By the same reasoning as above, this shows (19).  $\square$



FIGURE 10. Illustration: A green 7-tuple of nonintersecting lattice paths, corresponding to shape  $\lambda/\mu$ , and a red 7-tuple of nonintersecting lattice paths, corresponding to shape  $\sigma/\tau$ , constitute an *overlay* of nonintersecting lattice paths. Here,  $\sigma = (7, 4, 4, 3, 1, 1, 1)$ ,  $\tau = (3, 2, 2, 1)$ ,  $\lambda = \sigma + (1^{(7)})$  and  $\mu = \tau + (1^{(7)})$ . (Note that  $s_{\lambda/\mu} = s_{\sigma/\tau}$ .) The red and green paths are drawn with a slight offset for graphical reasons, the colour red is indicated by dashed lines. The picture also shows the Young tableaux corresponding to the red and green 7-tuples of nonintersecting lattice paths.



#### 4. PRODUCTS OF DETERMINANTS AS OVERLAYS OF LATTICE PATHS

In the following, all skew Schur functions are considered as functions of the same set of variables  $(x_1, \dots, x_n)$ . (Equivalently, all tableaux have entries from the set  $\{1, \dots, n\}$ , and all families of nonintersecting lattice paths have lower points on level 1 and upper points on level  $n$ ).

By (5) and the Lindström–Gessel–Viennot–interpretation of Young tableaux as nonintersecting lattice paths, we may view the product of two skew Schur functions as the generating function of pairs of  $m$ -tuples of nonintersecting lattice paths

$$s_{\lambda/\mu} \cdot s_{\sigma/\tau} = \sum_{(P_1, P_2)} \omega(P_1) \cdot \omega(P_2).$$

Here, the sum runs over all pairs  $(P_1, P_2)$ , where  $P_1$  is a  $\ell(\lambda/\mu)$ -tuple of nonintersecting lattice paths corresponding to the shape  $\lambda/\mu$  and  $P_2$  is a  $\ell(\sigma/\tau)$ -tuple of nonintersecting lattice paths corresponding to the shape  $\sigma/\tau$ . Imagine that the lattice paths of  $P_1$  and  $P_2$  are coloured red and green, respectively: This will give an *overlay* of lattice paths, see Figure 10 for an illustration.

Such overlays give rise to a bijective construction, which (to the best of our knowledge) was first used by Goulden [4]. The same construction was used in [2] to describe and prove a class of Schur function identities, special cases of which imply Dodgson's condensation formula and the Plücker relations.

We shall present this construction by way of an example: Consider skew shapes  $\lambda/\mu$  and  $\sigma/\tau$ , where  $\sigma = (7, 4, 4, 3, 1, 1, 1)$ ,  $\tau = (3, 2, 2, 1)$ ,  $\lambda = \sigma + (1^{(7)})$  and  $\mu = \tau + (1^{(7)})$ , see Figure 10 for an illustration.

Now consider the arcs, lower points and upper points of some pair  $(P_1, P_2)$  of 7-tuples of lattice paths, where  $P_1$  corresponds to shape  $\lambda/\mu$  and  $P_2$  corresponds to shape  $\sigma/\tau$ . Note that there may be arcs/points coloured both green *and* red. Such arcs/points will never be affected by the following constructions: We call them *uncoloured*; the *remaining* arcs/points (which are coloured *either* red *or* green) are called the *coloured* arcs/points.

We construct *bicoloured trails*

- connecting coloured points
- and using (only) coloured arcs

by the following algorithm:

We start at some coloured point  $s$  and identify the *unique* coloured arc  $a$  incident with  $s$  which is *of the same colour* as  $s$ . Then we follow the lattice path starting in  $a$  in the implied direction (i.e., either up/right if  $s$  is a lower point, or down/left if  $s$  is an upper point).

Whenever we meet *another* path on our way (necessarily, this path is of the other colour), we “change colour and direction”, i.e., we follow this new path *and* change the direction (i.e., if we were moving up/right along the old path, we move down/left along the new path, and vice versa). Note that such change of colour and orientation might also occur at the very beginning: For instance, if  $s$  is a green upper point, but there are two red arcs incident with  $s$ , then we follow the red arc in the up/right direction.

We stop if there is no possibility to go further, i.e., if we end in another coloured point.

Figure 11 illustrates this construction (see also [2]).

The following observations are immediate from the construction:

**Observation 3 (Bicoloured trails always exist).** *For every coloured point  $s$ , there exists a bicoloured trail starting at  $s$ .*

**Observation 4 (Bicoloured trail can never cross).** *Bicoloured trails may have lattice points in common (they may intersect), but they can never cross (see Figure 12).*

Now consider some bicoloured trail  $b$  in the overlay of nonintersecting lattice paths  $(P_1, P_2)$ : Changing colours (green to red and vice versa)

- of both ending points of  $b$

FIGURE 11. The picture shows the bicoloured trails (as thick grey trails with rounded corners) for the example from Figure 10.

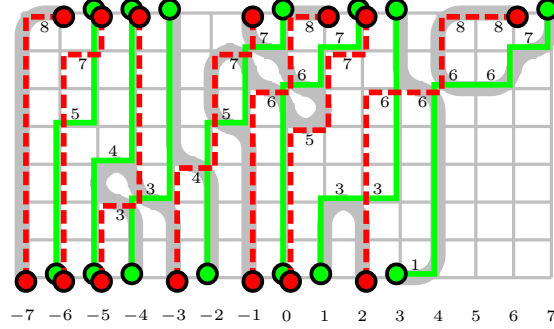


FIGURE 12. Illustration: Bicoloured trails can never cross. Since bicoloured trails never use arcs coloured both red *and* green, a meeting point of bicoloured trails can (up to interchanging colours red and green) only occur in the situations shown below. By construction, the bicoloured trails necessarily run as indicated by the grey lines.



- and of all arcs of  $b$

gives a new overlay of nonintersecting lattice paths  $(P'_1, P'_2)$  (with different lower/upper points, see Figure 13). Clearly, we have:

**Observation 5 (Recolouring bicoloured trails is a weight preserving involution).** *The recolouring of a bicoloured trail  $b$  in an overlay of nonintersecting lattice paths  $(P_1, P_2)$  is an involutive operation, i.e., if we obtain the overlay  $(P'_1, P'_2)$  by recolouring  $b$  in  $(P_1, P_2)$ , then recolouring  $b$  again in  $(P'_1, P'_2)$  yields the original  $(P_1, P_2)$ . Moreover, this operation preserves the respective weights, i.e.,*

$$\omega(P_1) \cdot \omega(P_2) = \omega(P'_1) \cdot \omega(P'_2).$$

Note that the operation of recolouring bicoloured trails changes the colours (red/green) of coloured lower and/or upper points (which implies a change of the corresponding shapes, see Figure 13). We want to encode this change in a convenient way: Imagine that all lower/upper points are arranged on a circle (see Figure 14). Assign to coloured point  $s$  the *radial orientation* (with respect to this circle)

- *inwards*, if  $s$  is a red upper point or a green lower point,
- *outwards*, if  $s$  is a green upper point or a red lower point.

FIGURE 13. Illustration. Recolouring two bicoloured trails (indicated by thick grey lines) from Figure 11 changes the colour of lower and/or upper points, thus changing the corresponding shape (shown below the paths).

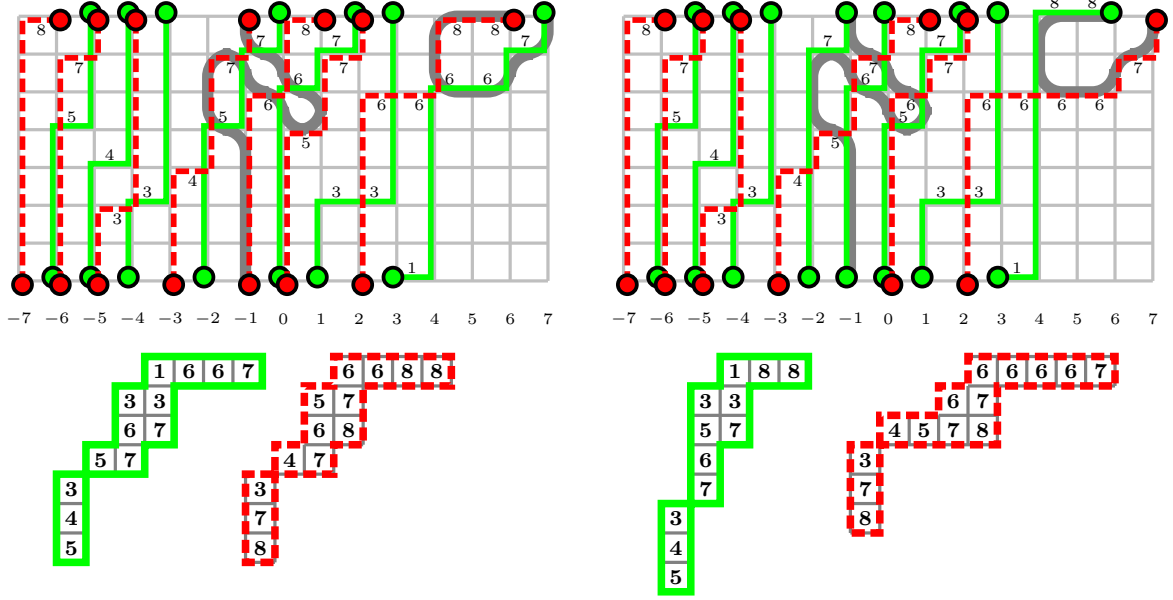
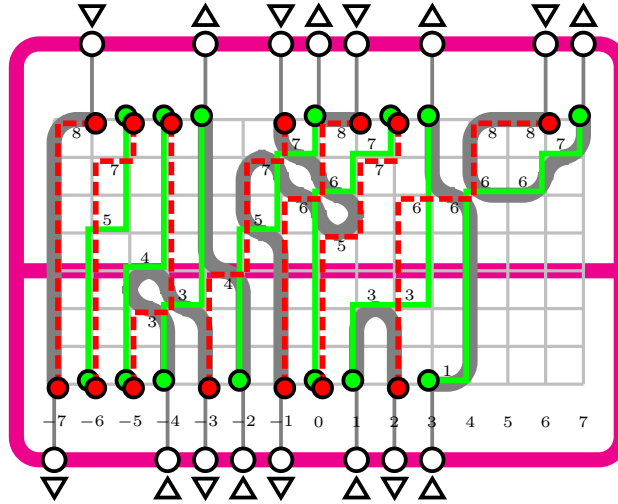


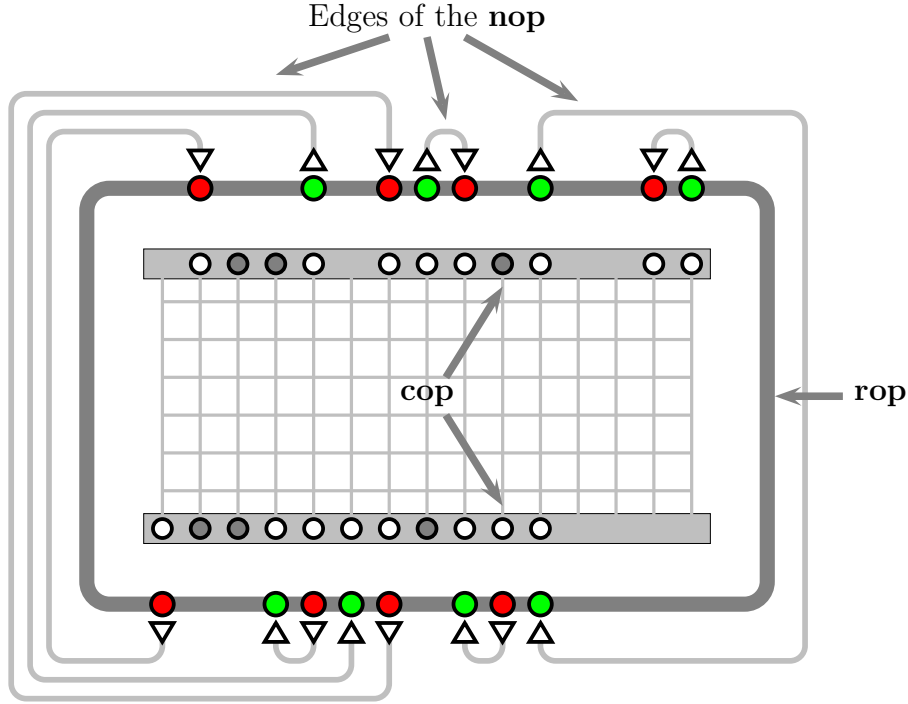
FIGURE 14. The “radial orientation” (indicated in the picture by triangles) of coloured points depends on the position (upper or lower) and colour (red or green) of the points.



See Figure 14. From the construction of bicoloured trails, the following is immediate:

**Observation 6 (Bicoloured trails connect points of different radial orientation).** *Bicoloured trails never connect points of the same radial orientation (i.e., two points oriented both inwards or both outwards).*

FIGURE 15. Coloured points may be green or red: The pattern of radial orientations **rop** (indicated by inward/outward pointing triangles) encodes the actual colours of the coloured points in the **cop** (indicated by white circles, the uncoloured points appear as grey circles) and thus determines the corresponding shapes  $\lambda/\mu$  and  $\sigma/\tau$ . The picture illustrates this for the example from Figure 13: The bicoloured trails constitute a *perfect noncrossing oriented matching* (**nop**), whose edges are indicated by grey arcs.



Clearly, we may “forget” the *actual* colours (red or green) of the coloured points, if we remember instead the pattern of radial orientations: The situation is completely determined by

- the geometric positions of the coloured and uncoloured lower and upper points, we call this piece of information the *configuration of (lower/upper) points* (short: **cop**),
- together with the pattern of radial orientation; we call this piece of information the *radial orientation of (coloured lower/upper) points* (short: **rop**).

Figure 15 illustrates this.

Note that for all **cops**, the number of coloured *upper* points plus twice the number of uncoloured *upper* points equals the number of coloured *lower* points plus twice the number of uncoloured *lower* points.

We call a **rop** *admissible* if it has the same number of inwardly/outwardly oriented points. *Every* admissible **rop** determines together with the corresponding **cop** a certain colouring (green and red) of lower/upper points, which represents a certain product of

two skew Schur functions

$$s_{\lambda/\mu} \cdot s_{\sigma/\tau},$$

where

- $\lambda/\mu$  is determined by the uncoloured points and the green points,
- $\sigma/\tau$  is determined by the the uncoloured points and the red points.

Note that there might be no overlay of families of nonintersecting lattice paths that connect these points (if, for instance, the  $i$ -th green upper point lies to the left of the  $i$ -th green lower point; this would correspond to an  $i$ -th row of length  $< 0$  in the corresponding Ferrers diagram: In this case, the corresponding skew Schur function  $s_{\lambda/\mu}$  is zero).

But if there *is* an overlay of families of nonintersecting lattice paths that connect the green and red points, then we may imagine that the **rop** corresponding to this overlay is arranged on a perfect circle: Observations 3, 4 and 6 imply that if we draw a straight line connecting two points in the **rop** whenever the corresponding coloured points are connected by a bicoloured trail, then we will obtain a **noncrossing oriented perfect matching** (short: **nop**)  $\mathbf{m}$ , i.e.:

- Every coloured point is incident with an edge in  $\mathbf{m}$ ,
- Every edge in  $\mathbf{m}$  connects points of *different radial orientation*,
- No two edges in  $\mathbf{m}$  do *cross* (in the geometric realization as straight lines connecting points on a circle).

In particular, this implies:

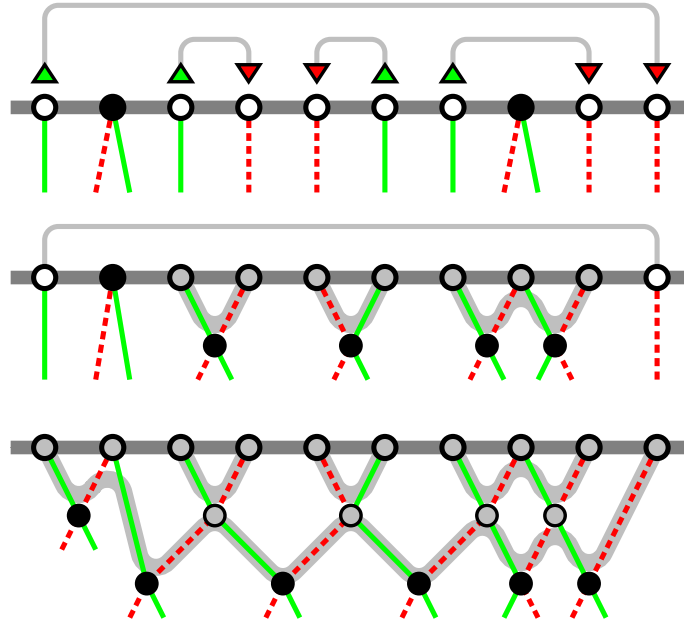
**Observation 7 (Bicoloured trails span equal numbers of inward and outward directed points).** *Assume  $p$  and  $q$  are coloured points in an overlay of nonintersecting lattice paths which are connected by some bicoloured trail. Then the corresponding **rop** is divided in two parts by the points corresponding to  $p$  and  $q$ : In each of these parts, the number of points directed inwards must equal the number of points directed outwards.*

*Stated otherwise: Let  $\mathbf{m}$  be a **nop** for a **rop**  $\mathbf{r}$ . An arbitrary edge  $e$  in  $\mathbf{m}$  divides  $\mathbf{r}$  into two parts, each of which must contain equal numbers of inward and outward oriented points.*

We conclude our preparatory considerations with the following observation:

**Observation 8 (Admissible matchings always can be realized by overlays of nonintersecting lattice paths).** *For every pair  $(\mathbf{c}, \mathbf{r})$ , where  $\mathbf{c}$  is a **cop** and  $\mathbf{r}$  is an admissible **rop** for  $\mathbf{c}$ , there exists a pair of shapes  $(\lambda/\mu, \sigma/\tau)$  characterized by  $(\mathbf{c}', \mathbf{r})$ , which has the same upper and lower uncoloured, green and red points as  $(\mathbf{c}, \mathbf{r})$  in the same order (i.e., only the geometric position of the points may differ), such that every **nop**  $\mathbf{m}$  in  $\mathbf{r}$  can be realized by an overlay of nonintersecting lattice paths corresponding to  $(\lambda/\mu, \sigma/\tau)$ : Maybe the best way to conceive this is by looking at pictures, see Figure 16 and Figure 17.*

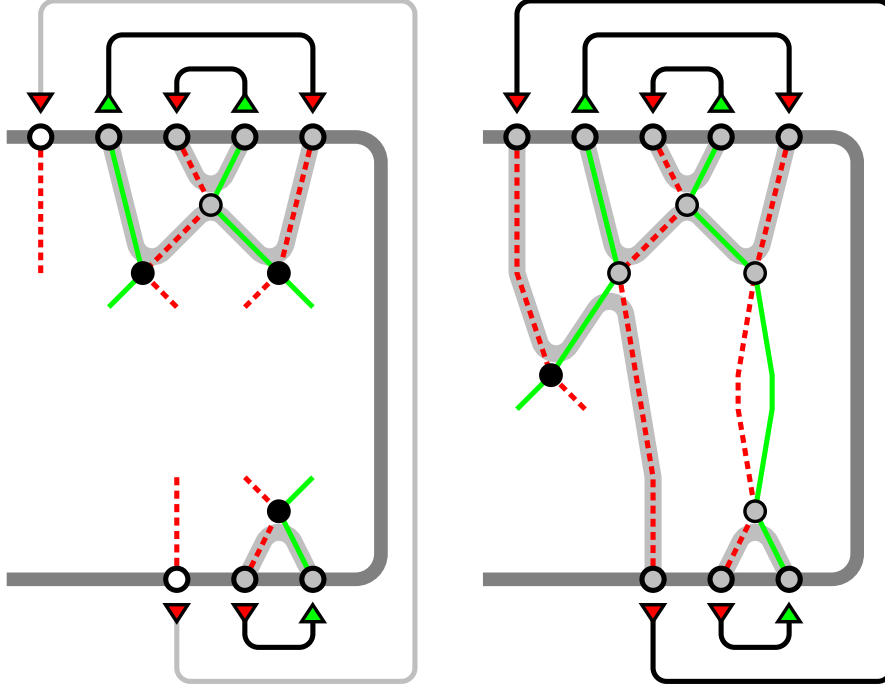
FIGURE 16. Illustration: Realizations of matchings. Assume we want to realize a *partial nop* for some subset  $S$  of *coloured* upper points which are *consecutive* in the corresponding *rop*. In the corresponding *cop*, there might be uncoloured points which are interspersed between the coloured points. As an example, consider the partial *nop* indicated in the upper picture. Imagine that the red and green paths are threads dangling down from the respective points: Note that *two* threads are dangling down from *uncoloured points* (shown as black circles), while only *one* thread is dangling down from *coloured points* (shown as white circles). Repeat the following step until there are no more coloured points: If two coloured points  $p_1, p_2$  are connected by an edge  $e$  of the partial *nop*, and all points between  $p_1$  and  $p_2$  (if any) are *uncoloured*, then arrange the threads dangling down from the points  $p_1, \dots, p_2$  such that they alternate in colour and tie together with knots the first and second, the third and fourth, etc., of these threads. View these knots as the new uncoloured points and simply *forget* the points  $p_1, \dots, p_2$ : Forgotten points are indicated by grey circles. The middle picture shows an intermediate state, where three edges of the partial *nop* are realized by bicoloured trails (shown as thick grey lines). The lower picture shows the final state, where there are no more coloured points, and all edges of the partial *nop* are *realized* by bicoloured trails. It is clear that the same algorithm realizes partial *nops* for subsets of *consecutive coloured* lower points.



## 5. APPLICATIONS: CLASSICAL AND NEW DETERMINANTAL IDENTITIES

The simple idea for all the identities considered in the rest of this paper could be stated in an *abstract* manner as follows: Assume some fixed *cop*  $\mathbf{c}$ .

FIGURE 17. Illustration: Realizations of matchings, 2nd part. Assume that all maximal partial **nops** on subsets of *consecutive coloured* lower or *consecutive coloured* upper points already have been realized, so now we have to realize edges connecting a lower point to an upper point where there is no coloured point between them (in the right half of the circular arrangement of points). The left picture indicates this situation: The edges already realized are shown as black lines. As in Figure 16, coloured points are shown as white circles, uncoloured points as black circles and forgotten points as grey circles. Obviously, by “tying together” threads of different colours (as in Figure 16) combined with “weaving together” threads of the same colour, we can realize the edge (shown as grey arc) that connects these two coloured points. It is clear that this algorithm indeed gives “topological” bicoloured trails corresponding to the **nop**, and it is also clear, that the “topological” situation can be implemented with lattice paths for appropriately chosen shapes (with large enough distances between the upper points and lower points).



- The set  $S$  of *all* overlays of nonintersecting lattice paths corresponding to  $\mathbf{c}$  and some fixed admissible **rop**  $\mathbf{r}$  corresponds to the set of *all* terms in the product  $s_{\lambda/\mu} \cdot s_{\sigma/\tau}$ , where the pair of shapes  $(\lambda/\mu, \sigma/\tau)$  corresponds to  $(\mathbf{c}, \mathbf{r})$ .
- The relation “corresponds to the same **nop** as” is an equivalence relation on  $S$ . Stated otherwise,  $S$  is *partitioned* into *matching classes* which are determined by the respective **nops**  $\mathbf{m}_1, \mathbf{m}_2, \dots$  of  $\mathbf{r}$ :

$$S = S_{\mathbf{m}_1} \cup S_{\mathbf{m}_2} \cup \dots, \text{ where } S_{\mathbf{m}_i} \cap S_{\mathbf{m}_j} = \emptyset \text{ for } i \neq j.$$

(Figure 18 visualizes this concept.)



- Let  $\mathbf{m}$  be a fixed **nop** in  $\mathbf{r}$ , and let  $\{e_1, \dots, e_k\}$  be a fixed set of edges of  $\mathbf{m}$ : Then the *recolouring* of the bicoloured paths  $\{b_1, b_2, \dots, b_k\}$  corresponding to  $\{e_1, \dots, e_k\}$  in  $S_{\mathbf{m}}$  effectuates a *weight-preserving* involution

$$S_{\mathbf{m}} \leftrightarrow S'_{\mathbf{m}},$$

where  $S'$  is the set of *all* overlays of nonintersecting lattice paths corresponding to  $(\mathbf{c}, \mathbf{r}')$ , where  $\mathbf{r}'$  is the **rop** obtained from  $\mathbf{r}$  by reversing the orientation of the points which are incident with the edges  $\{e_1, \dots, e_k\}$ . Note that except for this reversing of orientations of *points*, the **nop**  $\mathbf{m}$  is *unchanged*: Nevertheless, we will call this operation the *reversing of edges*  $\{e_1, \dots, e_k\}$  in  $\mathbf{m}$ .

- If we succeed in “glueing together” such *involutions for matching classes* such that we obtain a *weight preserving bijection*

$$S_1 \cup S_2 \cup \dots \leftrightarrow S'_1 \cup S'_2 \cup \dots,$$

where  $\{S_1, S_2, \dots\}$  and  $\{S'_1, S'_2, \dots\}$  are two families of sets of overlays corresponding to the two families

$$\begin{aligned} & - \{(\lambda_1/\mu_1, \sigma_1/\tau_1), (\lambda_2/\mu_2, \sigma_2/\tau_2), \dots\} \\ & - \text{and } \{(\lambda'_1/\mu'_1, \sigma'_1/\tau'_1), (\lambda'_2/\mu'_2, \sigma'_2/\tau'_2), \dots\} \end{aligned}$$

of pairs of shapes, then this bijection clearly translates to an identity involving sums of products of (skew) Schur functions

$$s_{\lambda_1/\mu_1} \cdot s_{\sigma_1/\tau_1} + s_{\lambda_2/\mu_2} \cdot s_{\sigma_2/\tau_2} + \dots = s_{\lambda'_1/\mu'_1} \cdot s_{\sigma'_1/\tau'_1} + s_{\lambda'_2/\mu'_2} \cdot s_{\sigma'_2/\tau'_2} + \dots.$$

The crucial point is the “glueing together” of involutions for matching classes. Clearly, this amounts to a consistent *rule* which identifies for every pair  $(\mathbf{r}, \mathbf{m})$  (where  $\mathbf{r}$  is a **rop** and  $\mathbf{m}$  is a **nop** in  $\mathbf{r}$ ) a *family*  $\{E_1, \dots, E_k\}$  of sets of edges to be *reversed*, thus relating  $(\mathbf{r}, \mathbf{m})$  to  $(\mathbf{r}'_1, \mathbf{m}), \dots, (\mathbf{r}'_k, \mathbf{m})$ , such that the iteration of this “edge-reversing procedure” yields a “bipartite substructure”, see Figure 18. We call such rule a *recolouring scheme*. In the following, we shall illustrate this abstract concept by several concrete examples.

**5.1. Dodgson’s condensation, revisited and generalized.** Recall Dodgson’s condensation formula (8), or rather its Schur function equivalent (11). Given our above preparations, Figure 19 contains the *proof* of (11)!

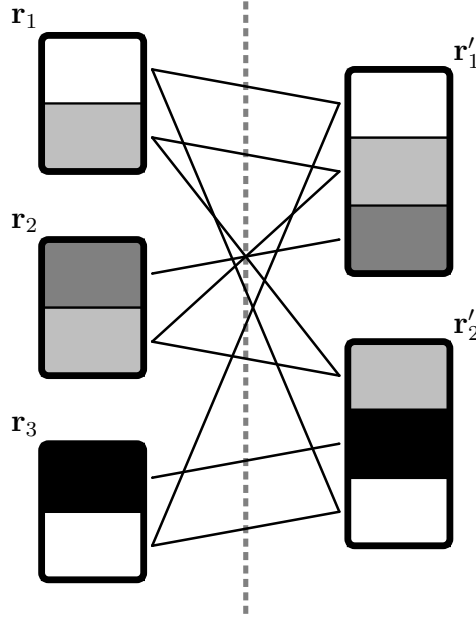
In order to see this, consider once again a special case: Let  $\lambda = (\lambda_1, \dots, \lambda_6) = (9, 7, 5, 3, 3, 1)$ ; for convenience, we denote  $(\lambda_2, \dots, \lambda_5)$  by  $\sigma$ . Dodgson’s formula starts with the product of Schur functions

$$s_{\lambda} \cdot s_{\sigma} = s_{\lambda} \cdot s_{\sigma + (-1^{(5)}) / (-1^{(5)})},$$

which by the Lindström–Gessel–Viennot–interpretation appears as generating function of overlays of nonintersecting lattice paths. See Figure 20, where the involutions visualized in Figure 19 are “specialized” to this concrete example. These weight-preserving involutions immediately imply (11), and it is obvious that the argument is valid not only for our special example, but in full generality, whence (by the reasoning following Corollary 1) we have proved (11) (and thus (8)).  $\square$

For the proof of Dodgson’s condensation formula, we used the following simple *recolouring scheme*: “Fix some nonempty subset  $S$  of coloured points of the same orientation (i.e., all points in  $S$  are either all outwards oriented or all inwards oriented), and in *all*

FIGURE 18. Illustration: The picture visualizes the situation where a *recolouring scheme* amounts to a weight preserving bijection between overlays corresponding to **rops**  $\{\mathbf{r}_1, \mathbf{r}_2, \mathbf{r}_3\}$  and  $\{\mathbf{r}'_1, \mathbf{r}'_2\}$ , respectively. In the picture it is assumed that there are only 4 **nops** for these **rops**, which are indicated by different shades of grey (white, light grey, grey and black). The crucial point is that the recolouring scheme assigns every **nop** to a “bipartite substructure” with bipartition classes *of the same size* (the edges of these “bipartite substructures” are shown as thin black lines). The simplest case of such “bipartite substructure” appears for the black **nop**  $\mathbf{m}_{\text{black}}$ : There is a *mapping* taking  $(\mathbf{r}_3, \mathbf{m}_{\text{black}})$  to  $(\mathbf{r}'_1, \mathbf{m}_{\text{black}})$  and vice versa. However, this is not the only possibility: Note that, for example, every white **nop**  $\mathbf{m}_{\text{white}}$  is related to *two* instances of  $\mathbf{m}_{\text{white}}$ : The corresponding “bipartite substructure” has bipartition classes  $\{(\mathbf{r}_1, \mathbf{m}_{\text{white}}), (\mathbf{r}_3, \mathbf{m}_{\text{white}})\}$  and  $\{(\mathbf{r}'_1, \mathbf{m}_{\text{white}}), (\mathbf{r}'_2, \mathbf{m}_{\text{white}})\}$  (both of size 2).



**nops** always reverse all edges incident with a point in  $S$ . We call this rule the *Dodgson recolouring scheme*.

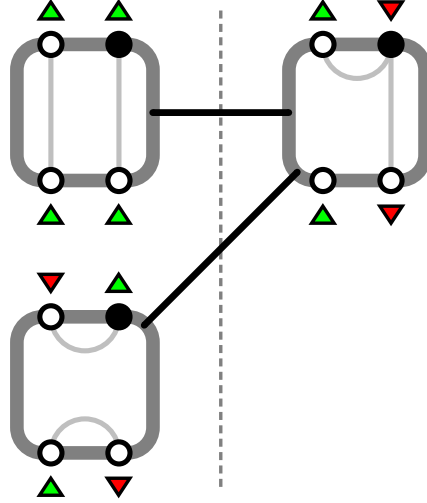
The following Lemma and its proof are a reformulation of [2, Lemma 15]):

**Lemma 1.** *Except for degenerate cases, the Dodgson recolouring scheme always yields a Schur function identity.*

*Proof.* Clearly, the Dodgson recolouring scheme unambiguously identifies for every **nop** the (single set of) edges to be reversed. The following proof is merely a clarification of the statement:

Let  $\lambda/\mu$  and  $\sigma/\tau$  be two skew shapes and consider the **cop**  $\mathbf{c}$  which corresponds to  $(\lambda/\mu, \sigma/\tau)$ . Without loss of generality, let  $S$  be a nonempty subset of *inwards* oriented points in  $\mathbf{c}$ .

FIGURE 19. Illustration: Graphical proof of Dodgson's condensation formula. The picture shows the three **rops** that may appear if the bicoloured path starting in the rightmost coloured upper point  $s$  (drawn as black circle) is recoloured. Note that there is only *one* **nop** (indicated by grey lines) for the **rops** in the left half of the picture, while there are *two* **nops**  $\mathbf{m}_1, \mathbf{m}_2$  for the **rop** in the right half of the picture (the edges incident with  $s$  in  $\mathbf{m}_1$  and  $\mathbf{m}_2$  are indicated by grey lines). The involution effectuated by the recolouring scheme is indicated by black lines connecting the respective **rops**, each of which represents a product of skew Schur functions.



Let  $V$  be the set of *all* admissible **rops** for  $\mathbf{c}$  where *all* points in  $S$  have the *same* orientation. Consider the graph  $G$  with vertex  $V$ , where two vertices  $v_1, v_2$  are connected by an edge if and only if there exists a **nop**  $\mathbf{m}$  for  $v_1$  such that  $v_2$  is obtained by applying the Dodgson recolouring scheme (i.e., reverse the edges in  $\mathbf{m}$  which are incident with a point in  $S$ ). Clearly, this graph  $G$  is *bipartite*:  $V = I \cup O$ , where  $I$  is the subset of  $V$  with all points in  $S$  oriented *inwards* and  $O$  is the subset of  $V$  with all points in  $S$  oriented *outwards*, and there is no edge connecting two vertices of  $I$  or two vertices of  $O$  (see again Figure 19, where the bipartite structure is indicated by a dashed line separating the left and right half of the picture).

Assume that graph  $G$  has a connected component  $Z$  with at least 2 vertices (if there is no such component, we call this a *degenerate case*). Then we have the following identity for skew Schur functions:

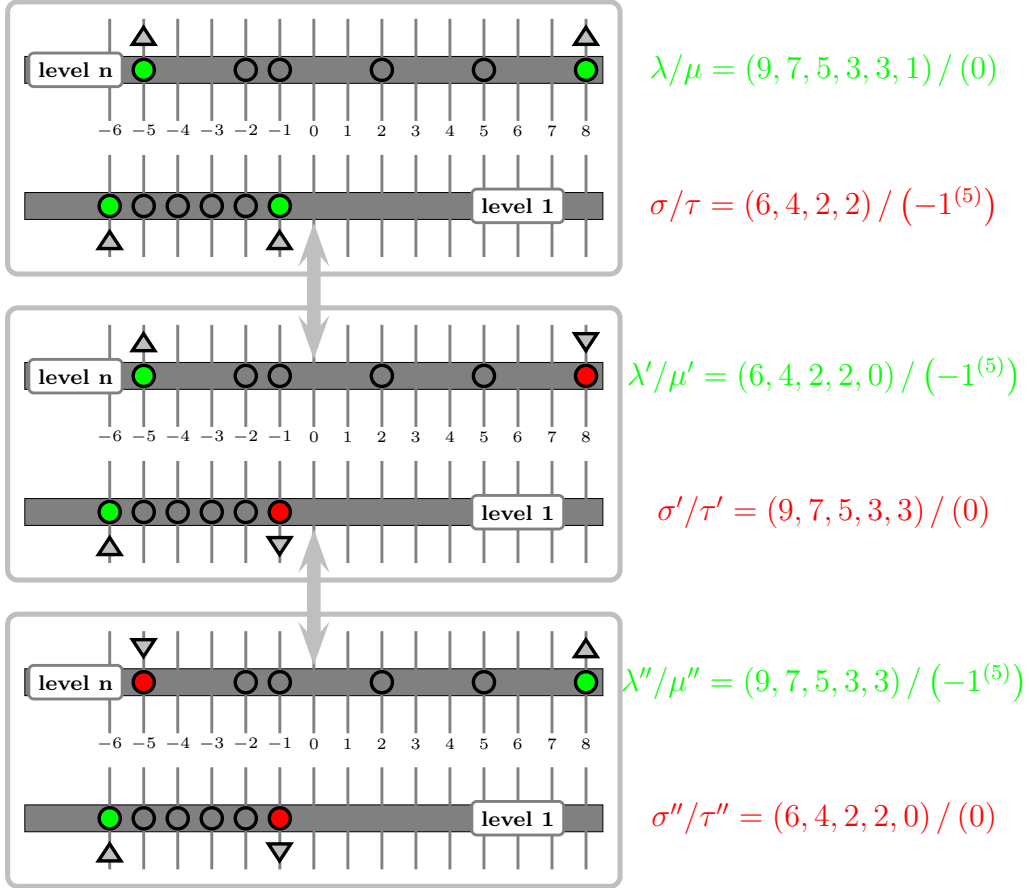
$$\sum_{(\lambda/\mu, \sigma/\tau) \in Z_I} s_{\lambda/\mu} \cdot s_{\sigma/\tau} = \sum_{(\lambda'/\mu', \sigma'/\tau') \in Z_O} s_{\lambda'/\mu'} \cdot s_{\sigma'/\tau'}, \quad (20)$$

where  $Z_O$  and  $Z_I$  denote the sets of pairs of skew shapes corresponding to  $(\mathbf{c}, x)$  for  $x \in O$  and  $x \in I$ , respectively.  $\square$

We illustrate Lemma 1 by the following generalization of Dodgson's condensation, which might be new. Consider the **rop** with  $k$  upper and  $k$  lower points ( $k > 1$ ) which are all green, and always recolour the bicoloured path starting in the rightmost upper point

FIGURE 20. Illustration: Dodgson's condensation formula, by example. The pictures show the positions of lower and upper points of the overlays corresponding to shapes derived from  $\lambda/\mu = (9, 7, 5, 3, 3, 1) / (0)$  and  $\sigma/\tau = (6, 4, 2, 2) / (-1^{(5)})$ . In the upper picture, all coloured points are green, and the bicoloured path  $b$  starting in the rightmost upper point  $s = (8, n)$  *must* have the rightmost lower point  $(-1, 1)$  as its other ending point. Recolouring  $b$  leads to the middle picture. Here, the bicoloured path starting in  $s$  has *two* possibilities: Its other ending point might be  $(-1, 1)$  again, but also the leftmost upper point  $(-5, n)$  is possible. For the latter case, recolouring the bicoloured path connecting  $s$  and  $(-5, n)$  leads to the lower picture. Now, as in the upper picture, the bicoloured path starting in  $s$  *must* have  $(-5, n)$  again as its other ending point. By the above reasoning, this shows immediately the following specialization of (11):

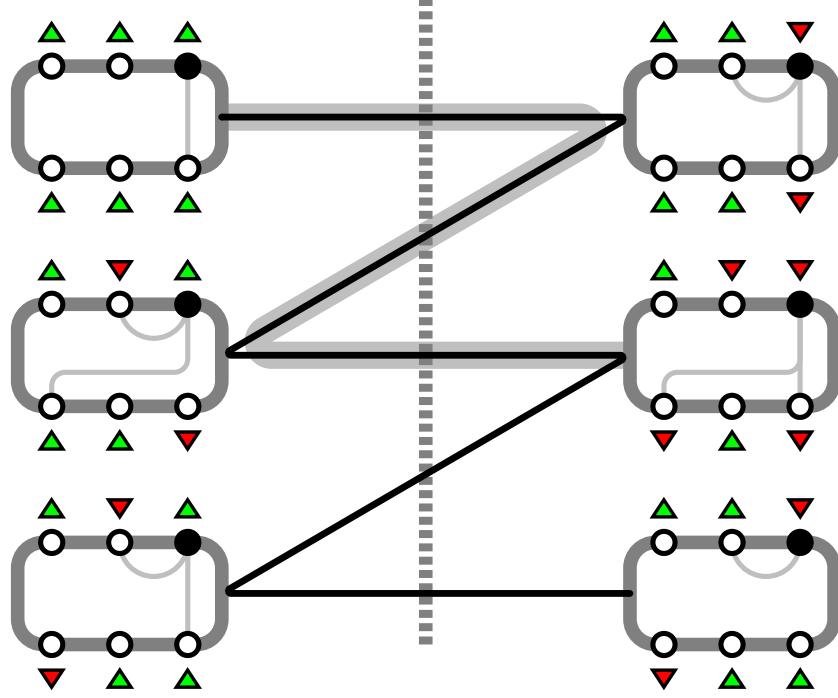
$$s_{\lambda/\mu} \cdot s_{\sigma/\tau} + s_{\lambda''/\mu''} \cdot s_{\sigma''/\tau''} = s_{\lambda'/\mu'} \cdot s_{\sigma'/\tau'}$$



( $k = 2$  corresponds to Dodgson's condensation, see Figure 19; the cases  $k = 3$  and  $k =$  are depicted in Figure 20 and 21).

**Theorem 2.** Let  $a$  be an  $(m + k) \times (m + k)$ -matrix, and let  $1 \leq i_1 < i_2 < \dots < i_k \leq m + k$  and  $1 \leq j_1 < j_2 < \dots < j_k \leq m + k$  be (the indices of)  $k$  fixed rows and  $k$  fixed

FIGURE 21. Dodgson's recolouring rule, where the set  $S$  consists only of the rightmost coloured upper point (drawn as black circle), applied to 3 upper/lower points.



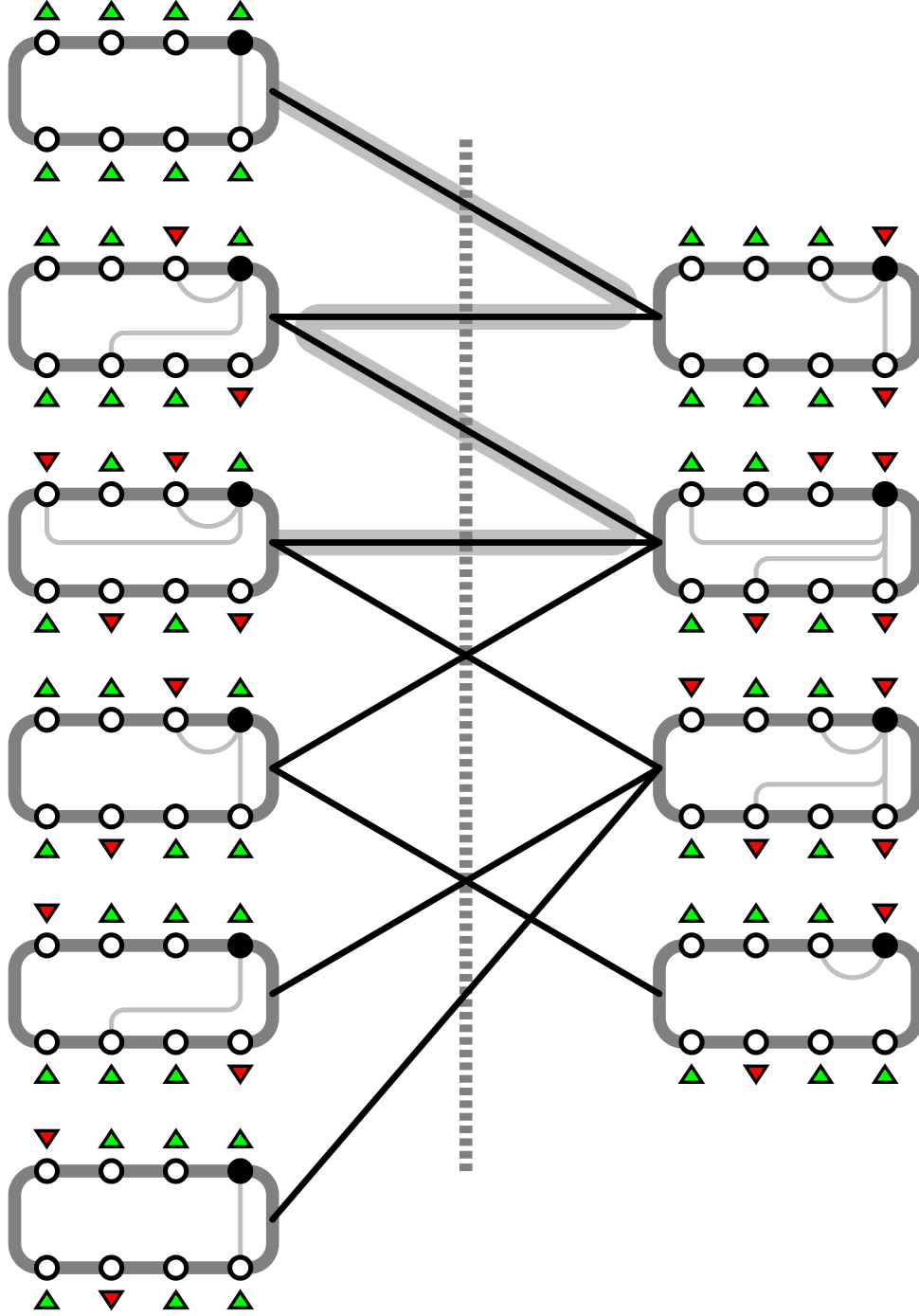
columns, respectively, of  $a$ . Denote the sets of these (indices of) rows and columns by  $R$  and  $C$ , respectively.

Let  $E := \{j_2, j_4, \dots, j_{2 \cdot \lfloor k/2 \rfloor}\}$  and  $O := \{i_1, i_3, \dots, i_{2 \cdot \lceil k/2 \rceil - 1}\}$  be the sets of odd fixed row indices and of even fixed column indices, respectively. Then we have:

$$\sum_{\substack{S \subseteq E, \\ T \subseteq O, \\ |S|=|T|}} \left| (a)_{\overline{T}, \overline{S}} \right| \cdot \left| (a)_{\overline{R \setminus T}, \overline{C \setminus S}} \right| = \sum_{\substack{S \subseteq E, \\ T \subseteq O, \\ |S|=|T|-1}} \left| (a)_{\overline{T}, \overline{S \cup \{j_1\}}} \right| \cdot \left| (a)_{\overline{R \setminus T}, \overline{C \setminus (S \cup \{j_1\})}} \right|. \quad (21)$$

*Proof.* We shall prove the Schur function identity equivalent to (21): Note that the corresponding **cop** shows  $m + k$  lower points, of which  $k$  are coloured, and  $m + k$  upper points, of which  $k$  are coloured. As always, we concentrate on the coloured points: Denote the upper coloured points by  $t_1, t_2, \dots, t_k$ , and the lower coloured points by  $s_1, s_2, \dots, s_k$  (counted from the right, as always). Consider the **rop** where *all* coloured points are *green* (see the uppermost configuration in the left parts of Figures 20 and 21): This **rop** corresponds to the summand for  $S = T = \emptyset$  in the left-hand side of (21). Clearly, the other end of a bicoloured path starting in the rightmost upper point  $t_1$  must either be in the set  $O := \{s_1, s_3, \dots, s_{2 \cdot \lceil k/2 \rceil - 1}\}$  or in the set  $E := \{t_2, t_4, \dots, t_{2 \cdot \lfloor k/2 \rfloor}\}$ . Now observe that it is possible to recolour points  $s_1, t_2, s_3, t_4, \dots$  (in this order; these recolouring steps are indicated by thick grey lines in Figures 20 and 21) until we obtain the **rop** where *all* points in  $E \cup O$  are coloured red. (Note that in this **rop**,  $t_1$  is green

FIGURE 22. Dodgson's recolouring rule, where the set  $S$  consists only of the rightmost coloured upper point (drawn as black circle), applied to 4 upper/lower points.



if  $k$  is even, otherwise  $t_1$  is red.) Now it is easy to see that for an arbitrary choice of subsets  $S, T$ , where  $S \subseteq E \cup \{t_1\}$ ,  $T \subseteq O$  and  $|S| = |T|$ , by the recolouring of red upper and lower points in the appropriate order, we can obtain the situation where the set of red points is precisely the union  $S \cup T$ : This translates to the assertion.  $\square$

As an example, we state the determinantal identity corresponding to Figure 22 ( $k = 4$ ) for the special case where  $a$  is a  $4 \times 4$ -matrix (i.e.,  $m = 0$ ):

$$\begin{aligned} |a| = & \left| (a)_{1,1} \right| \cdot \left| (a)_{\overline{1}, \overline{1}} \right| + \left| (a)_{1,3,1,2} \right| \cdot \left| (a)_{\overline{1}, \overline{3}, \overline{1}, \overline{2}} \right| + \left| (a)_{1,3,1,4} \right| \cdot \left| (a)_{\overline{1}, \overline{3}, \overline{1}, \overline{4}} \right| + \left| (a)_{3,1} \right| \cdot \left| (a)_{\overline{3}, \overline{1}} \right| \\ & - \left| (a)_{1,2} \right| \cdot \left| (a)_{\overline{1}, \overline{2}} \right| - \left| (a)_{1,3,2,4} \right| \cdot \left| (a)_{\overline{1}, \overline{3}, \overline{2}, \overline{4}} \right| - \left| (a)_{3,2} \right| \cdot \left| (a)_{\overline{3}, \overline{2}} \right| \\ & - \left| (a)_{1,4} \right| \cdot \left| (a)_{\overline{1}, \overline{4}} \right| - \left| (a)_{3,4} \right| \cdot \left| (a)_{\overline{3}, \overline{4}} \right|. \end{aligned}$$

**5.2. (Generalized) Plücker relations.** There is a particularly simple special case of Lemma 1 (this is a reformulation of [2, Lemma 16]):

**Corollary 2.** *Let  $\mathbf{r}$  be the **rop** for the pair of shapes  $(\lambda/\mu, \sigma/\tau)$ , and assume that the orientation of the points in  $\mathbf{r}$  is alternating. Consider the set of all **rops** which arise by applying Dodgson's recolouring scheme (for some fixed nonempty set of points of the same orientation) to  $\mathbf{r}$  and denote the corresponding set of pairs of skew shapes by  $Q$ .*

*Then we have:*

$$s_{\lambda/\mu} \cdot s_{\sigma/\tau} = \sum_{(\lambda'/\mu', \sigma'/\tau') \in Q} s_{\lambda'/\mu'} \cdot s_{\sigma'/\tau'}. \quad (22)$$

*Proof.* Consider the **rop**  $\mathbf{r}'$  corresponding to some Schur function product  $s_{\lambda'/\mu'} \cdot s_{\sigma'/\tau'}$  from the right hand side of (22): By the combination of Observations 6 and 4, it is clear that re-applying the Dodgson recolouring scheme *must* give the **rop**  $\mathbf{r}$  corresponding to the Schur function product  $s_{\lambda/\mu} \cdot s_{\sigma/\tau}$ .  $\square$

We will use this Corollary for a proof of the Plücker relations (also known as Grassmann–Plücker syzygies, see [15], or as Sylvester's Theorem, see [12, section 137]). In addition to notation  $[m] := \{1, 2, \dots, m\}$  we introduce the notation

$$([m] + n) := \{n + 1, n + 2, \dots, n + m\}.$$

Moreover, for finite ordered sets  $X \subseteq S$  and  $Y$  with  $Y \cap S = \emptyset$ ,  $|Y| = |X|$ , we introduce the notation  $(S|_{\leftarrow Y}^{X \rightarrow})$  for the set  $S$  where the elements of  $X$  are replaced by the elements of  $Y$  in the same order, i.e., if ordered sets  $X$  and  $Y$  are given as  $X = (x_1, x_2, \dots)$  and  $Y = (y_1, y_2, \dots)$ , respectively, and  $S$  is given as

$$S = (s_1, \dots, s_{(k_1-1)}, x_1, s_{(k_1+1)}, \dots, s_{(k_2-1)}, x_2, s_{(k_2+1)}, \dots),$$

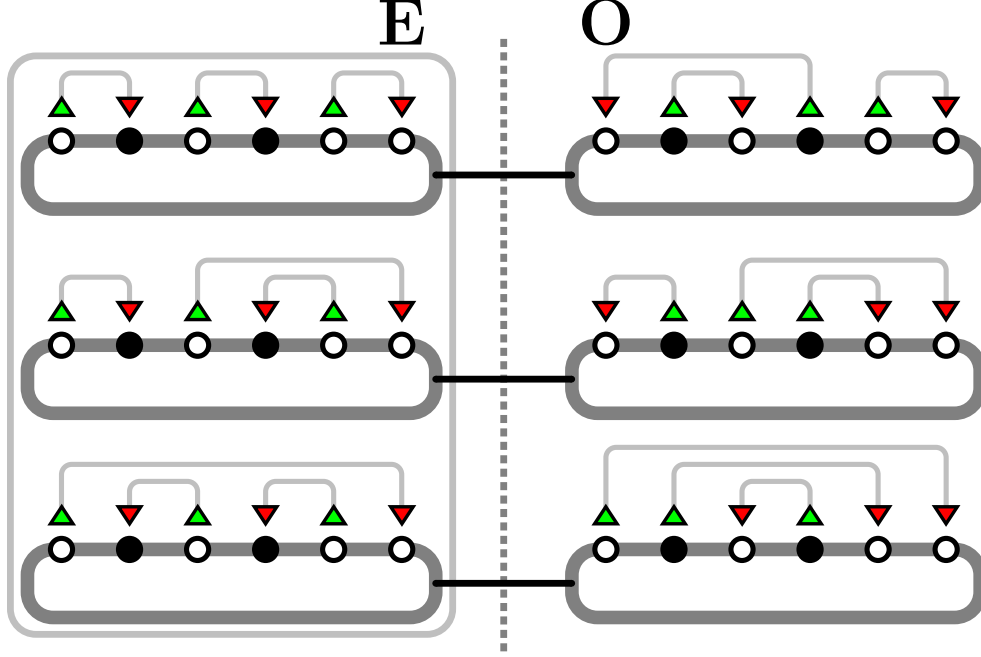
then ordered set  $(S|_{\leftarrow Y}^{X \rightarrow})$  is given as

$$(S|_{\leftarrow Y}^{X \rightarrow}) = (s_1, \dots, s_{(k_1-1)}, y_1, s_{(k_1+1)}, \dots, s_{(k_2-1)}, y_2, s_{(k_2+1)}, \dots).$$

**Theorem 3** (Plücker relations). *Let  $a = (a_{i,j})_{(i,j) \in [2m] \times [m]}$  be a  $2 \cdot m \times m$  matrix. Consider some fixed set  $R \subseteq [m]$ . Then we have*

$$\left| (a)_{[m], [m]} \right| \cdot \left| (a)_{[m], ([m]+m)} \right| = \sum_{\substack{S \subseteq ([m]+m), \\ |S|=|R|}} \left| (a)_{[m], ([m]|_{\leftarrow S}^{R \rightarrow})} \right| \cdot \left| (a)_{[m], ([2m] \setminus [m]|_{\leftarrow R}^{S \rightarrow})} \right|. \quad (23)$$

FIGURE 23. Illustration of the Plücker relation (23) for  $m = 3$ : The left part shows *three copies* of the **rop** considered in the proof of Theorem 3 with different **nops**; the right part shows the effect of recolouring the fixed points which are indicated by black circles. Note that there are *five* possible **nops** in this situation: For the upper and lower pictures, there are *two* **nops** which yield the same recolouring; these two **nops** are shown in the left and right parts of the pictures, respectively.



*Proof.* We shall prove a Schur function identity which is equivalent to (23): Consider

$$\lambda = ((2 \cdot m) \cdot (m - 1), (2 \cdot m - 2) \cdot (m - 1), \dots, 4 \cdot (n - 1), 2 \cdot (n - 1))$$

and

$$\sigma = ((2 \cdot m - 1) \cdot (m - 1), (2 \cdot m - 3) \cdot (m - 1), \dots, 3 \cdot (n - 1), (n - 1))$$

and assume that matrix  $(a)_{[m], [m]} = \mathbf{h}_\lambda$  and matrix  $(a)_{([m]+m), [m]} = \mathbf{h}_\sigma$ . It is clear that the **rop** corresponding to the pair of shapes  $(\lambda / (0), \sigma / (0))$  has only *upper* coloured points which alternate in orientation, see the uppermost configuration in the left part of Figure 23. Corollary 2 immediately translates to (the Schur function equivalent of) (23); see Figure 23 for an illustration.  $\square$

Note that the proof (which basically is *contained* in Figure 23!) implies an obvious generalization: Of course, there might be *uncoloured* points in the **cops** associated to the **rops** shown in Figure 23! Such uncoloured points amount to a slightly more general Schur function identity (in [5, (3.3)], this identity is stated by describing the situation with certain operations of Ferrers diagrams and proved by using the Plücker relations; the connection of this identity to the more general statements presented here was already explained *ad hoc* in [1]), or to a *common minor* in the products of determinants (as in Theorem 2):



**Theorem 4.** *Let  $a$  be an  $(m+k) \times (m+2 \cdot k)$ -matrix, and let  $1 \leq j_1 < j_2 < \dots < j_k \leq m+2 \cdot k$  be (the indices of)  $2 \cdot k$  fixed columns of  $a$ , and set  $A := \{j_1, \dots, j_k\}$  and  $O := \{j_{k+1}, \dots, j_{2 \cdot k}\}$ . Let  $A' := [m+2 \cdot k] \setminus A$  and  $O' := [m+2 \cdot k] \setminus O$ . Consider some fixed set  $R \subseteq A$ . Then we have:*

$$\left| (a)_{[m+k], A'} \right| \left| (a)_{[m+k], O'} \right| = \sum_{\substack{S \subseteq O, \\ |S|=|R|}} \left| (a)_{[m+k], (A'|_{\leftarrow S}^{R \rightarrow})} \right| \cdot \left| (a)_{[m+k], (O'|_{\leftarrow R}^{S \rightarrow})} \right|. \quad (24)$$

**5.3. Laplace expansion.** Assume we are given some **rop**  $\mathbf{r}$  with at least  $m$  lower points  $s_1, \dots, s_m$ . We introduce a new recolouring scheme: Fix lower points  $S := \{s_{i_1}, \dots, s_{i_k}\}$  in  $\mathbf{r}$  ( $k \leq m$ ). For every **nop**  $\mathbf{m}$ , reverse

- one of the edges of  $\mathbf{m}$  connecting *two consecutive* coloured upper points (we call such edge an upper *handle*), if there is one,
- else *all* the edges of  $\mathbf{m}$  starting at a point of  $S$ .

We call this the *Laplace recolouring scheme*: Applying this scheme for  $S = \{j\}$  (i.e.,  $k = 1$ ) to the **cop** with  $m$  upper and  $m$  lower points,  $m > 1$ , all of which are coloured green, implies the Laplace expansion of the  $m \times m$ -determinant by its  $j$ -th column

$$|a| = \sum_{i=1}^m (-1)^{i-j} \cdot |a_{i,j}| \cdot \left| (a)_{\overline{i}, \overline{j}} \right|. \quad (25)$$

As for Dodgson's condensation, Figure 24 contains the *proof*: The concrete example presented there illustrates the case  $m = 4$ ,  $j = 1$ , and generalizes to a general Schur function identity, which implies (25).  $\square$

For the generalization of Laplace's expansion (see [12, section 93]), we introduce the following notation: Let  $X = \{x_1, \dots, x_m\} \subset \mathbb{Z}$  be an ordered set, and let  $S = \{x_{i_1}, \dots, x_{i_k}\}$ ,  $k \leq m$ , be a subset. In this situation, we define

$$\Sigma_{S \subseteq X} := \sum_{j=1}^k i_j.$$

**Theorem 5** (Laplace's Theorem). *Let  $a = (a_{i,j})_{(i,j) \in [m] \times [m]}$  be an  $m \times m$ -matrix. Consider some fixed set  $I \subseteq [m]$ . Then we have*

$$|a| = \sum_{\substack{J \subseteq [m], \\ |J|=|I|}} (-1)^{\Sigma_{I \subseteq [m]} + \Sigma_{J \subseteq [m]}} \cdot \left| (a)_{I, J} \right| \cdot \left| (a)_{\overline{I}, \overline{J}} \right|. \quad (26)$$

*Proof.* As always, we consider the equivalent Schur function identity: The **rop** corresponding to the left-hand side of (26) consists of

- $m$  upper points, which are outward oriented,
- and  $m$  lower points, which are inward oriented

(stated otherwise: All  $2 \cdot m$  coloured points are green; see Figure 25 for an illustration). We may assume  $0 < |I| < m$  (otherwise, there is nothing to prove), i.e.,  $I$  corresponds to  $k$  lower points  $s_{i_1}, \dots, s_{i_k}$ ,  $0 < k < m$ .

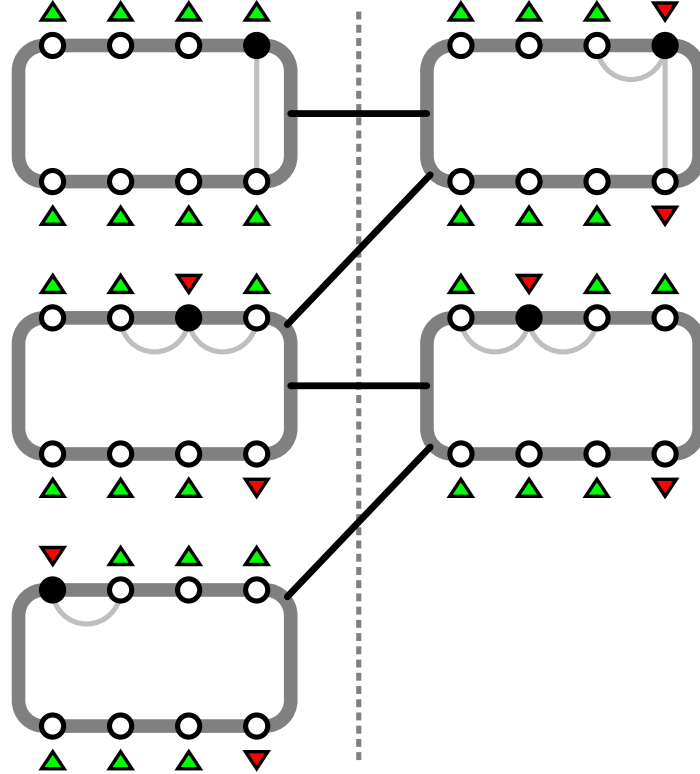
FIGURE 24. The proof of the Laplace expansion of the  $4 \times 4$ -determinant is contained in the pictures below. The starting point  $s$  of the bicoloured trail to be recoloured is indicated by a coloured circle, and the possible connections by bicoloured trails are indicated by grey arcs. Note that for some partition  $\lambda = (\lambda_1, \dots, \lambda_4)$ , the involutions (indicated in the pictures by thick black lines) imply that the generating function of the left half,

$$s_{(\lambda+(1^{(m)}))/1^{(4)}} \cdot s_{(0)} + s_{(\lambda+(1^{(m)}))\overline{2}} \cdot s_{(\lambda_2-1)} + s_{(\lambda+(1^{(m)}))\overline{4}} \cdot s_{(\lambda_4-3)},$$

is equal to the generating function of the right half,

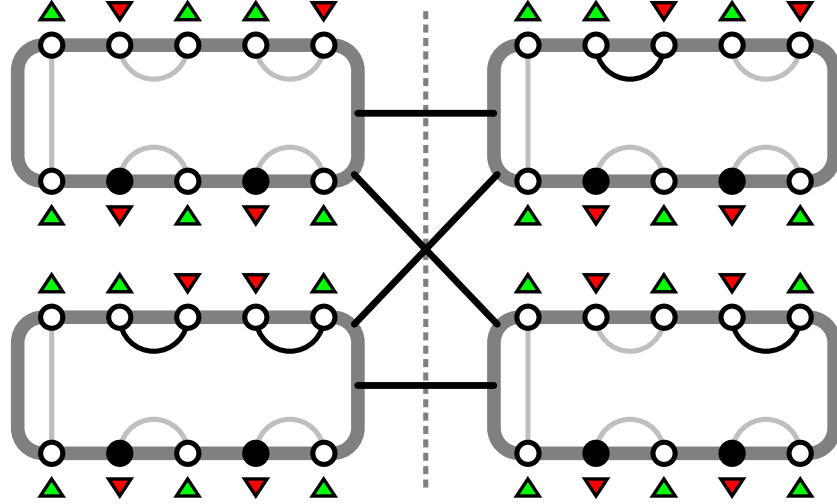
$$s_{(\lambda+(1^{(m)}))/1^{(4)}} \cdot s_{(0)} + s_{(\lambda+(1^{(m)}))\overline{2}} \cdot s_{(\lambda_2-1)} + s_{(\lambda+(1^{(m)}))\overline{4}} \cdot s_{(\lambda_4-3)}.$$

By the connections between minors of  $\mathbf{h}_{\sigma/\tau}$  and operations on partitions  $\sigma$  and  $\tau$  (which were explained before Corollary 1), this means  $|\mathbf{h}_\lambda| = |(\mathbf{h}_\lambda)_{\overline{1}, \overline{1}}| \cdot (\mathbf{h}_\lambda)_{1,1} - |(\mathbf{h}_\lambda)_{\overline{2}, \overline{1}}| \cdot (\mathbf{h}_\lambda)_{2,1} + |(\mathbf{h}_\lambda)_{\overline{3}, \overline{1}}| \cdot (\mathbf{h}_\lambda)_{3,1} - |(\mathbf{h}_\lambda)_{\overline{4}, \overline{1}}| \cdot (\mathbf{h}_\lambda)_{4,1}$ , which implies the Laplace expansion (by the first column).



Now we apply the Laplace recolouring scheme. Note that there *always* is an upper handle if there is an edge connecting two upper points. If there is more than one upper handle, the recolouring scheme does *not* describe a *mapping*, but a *multi-valued relation* on pairs  $(\mathbf{r}, \mathbf{m})$ , where  $\mathbf{r}$  is a **rop** and  $\mathbf{m}$  is a **nop** in  $\mathbf{r}$ : It is easy to see that nevertheless a *bipartite substructure* occurs (see Figure 18): Starting with some arbitrary but fixed pair  $(\mathbf{r}, \mathbf{m})$ , by the Laplace recolouring scheme all the pairs  $(\mathbf{r}'', \mathbf{m})$  which are obtained by reversing an *even* number of upper handles, end up in the same

FIGURE 25. Illustration of Laplace’s Theorem, for  $m = 5$  and  $J = \{2, 4\}$ : The lower points corresponding to  $J$  are indicated by black circles. The **nop** shown in the picture has two upper handles (edges connecting neighbouring upper points); handles that have been “reversed” (i.e., their end-points were recoloured) are drawn in black. The important point is that the same number of pairs (**rop**, **nop**) appears in the two bipartition classes (corresponding to the left and the right half of the picture); see also Figure 18 where this situation appears in a more “abstract” way.



bipartition class as  $(\mathbf{r}, \mathbf{m})$ : Clearly, these are of the same number as all the pairs  $(\mathbf{r}', \mathbf{m})$  which are obtained by reversing an *odd* number of upper handles (constituting the other bipartition class).  $\square$

Note that the same proof also works for **cops** which contain *uncoloured* points: This amounts to a slightly more general statement (see [12, section 148])

**Theorem 6.** *Let  $a$  be an  $(m+k) \times (m+k)$ -matrix, and let  $1 \leq i_1 < i_2 < \dots < i_m \leq m+k$  and  $1 \leq j_1 < j_2 < \dots < j_m \leq m+k$  be (the indices of)  $k$  fixed rows and  $k$  fixed columns of  $a$ . Denote the set of these (indices of) rows and columns by  $R$  and  $C$ , respectively. Consider some fixed set  $I \subseteq R$ . Then we have:*

$$|a| \cdot \left| (a)_{\overline{R}, \overline{C}} \right| = \sum_{\substack{J \subseteq C, \\ |J|=|I|}} (-1)^{\sum I R + \sum J \subseteq C} \cdot \left| (a)_{R, S} \right| \cdot \left| (a)_{\overline{R}, \overline{S}} \right|. \quad (27)$$

## REFERENCES

- [1] Markus Fulmek. Bijective proofs for Schur function identities. arXiv:0909.5334v1 [math.CO], 2009.
- [2] Markus Fulmek and Michael Kleber. Bijective proofs for Schur function identities which imply Dodgson’s condensation formula and Plücker relations. *Electron. J. Combin.*, 8(1):Research Paper 16, 22 pp. (electronic), 2001.
- [3] Ira M. Gessel and Xavier Viennot. Determinants, paths, and plane partitions. preprint, 1989.
- [4] Ian P. Goulden. Quadratic forms of skew Schur functions. *European J. of Combinatorics*, 9:161–168, 1988.

- [5] Dimitri Gurevich, Pavel Pyatov, and Pavel Saponov. Bilinear identities on Schur symmetric functions. *Journal of Nonlinear Mathematical Physics*, to appear, 2010. (also available as arXiv:0907.4292v2 [math.CO]) Status: <http://www.worldscinet.com/jnmp/mkt/archive.shtml?2010&17>.
- [6] C.G. Jacobi. De functionibus alternantibus earumque divisione per productum e differentiis elementorum conflatum. *J. Reine Angew. Math.*, 22:360–371, 1841.
- [7] Samuel Karlin. Coincident probabilities and applications to combinatorics. *J. Appl. Probab.*, 25A:185–200, 1988.
- [8] A.N. Kirillov. Completeness of states of the generalized Heisenberg magnet. *J. Soviet Math.*, 1987.
- [9] Michael Kleber. Plücker relations on Schur functions. *Journal of Algebraic Combinatorics*, 13:199–211, 2001.
- [10] B. Lindström. On the vector representation of induced matroids. *Bull. London Math. Soc.*, 5:85–90, 1973.
- [11] I.G. MacDonald. *Symmetric Functions and Hall Polynomials*. Oxford Science Publications, 2nd edition, 1995.
- [12] T. Muir. *A Treatise on the Theory of Determinants*. Longmans, Green and Co., 1933.
- [13] Bruce E. Sagan. *The Symmetric Group*. Springer, 2nd edition, 2000.
- [14] Issai Schur. *Über eine Klasse von Matrizen, die sich einer gegebenen Matrix zuordnen lassen*. PhD thesis, Berlin, 1901.
- [15] B. Sturmfels. *Algorithms in Invariant Theory*. Texts and Monographs in Symbolic Computation. Springer-Verlag, Wien, 1993.
- [16] N. Trudi. Intorno un determinante piu generale di quelle che suol dirsi determinante delle radici di una equazione, ed alle funzioni simmetriche complete di questo radici. *Rend. Accad. Sci. Fis. Mat. Napoli*, 3:121–134, 1864.

FAKULTÄT FÜR MATHEMATIK, NORDBERGSTRASSE 15, A-1090 WIEN, AUSTRIA

E-mail address: Markus.Fulmek@Univie.Ac.At

WWW: <http://www.mat.univie.ac.at/~mfulmek>